

In reliance thereon, the claims have not been amended.

The Official Action objects to the amendment filed November 4, 2002 because the change from cubic meters to cubic centimeters is alleged to be new matter, and the claims were rejected under §112, first paragraph, for the same reason. Reconsideration and withdrawal of the objection and rejection are respectfully requested.

The change from cubic meters to cubic centimeters corrects a typographical error and does not introduce new matter. This is supported by the application as filed and by extrinsic evidence presented herewith.

The specification as filed refers to JP 10-12969 on page 8, lines 11-16. The original specification characterized this reference as disclosing an impurity concentration in atoms per cubic meter. However, the reference actually discloses the same impurity concentration in atoms per cubic centimeter. A copy of this reference in Japanese accompanies this response. As may be seen in paragraph 0021, the impurity concentration is in atoms per cubic centimeter (the entire reference uses cubic centimeters; see paragraphs 0010, 0011, 0022, and Figure 4, for example). Accordingly, the specification as filed supports the correction to cubic centimeters.

Further, in this art impurity concentration is typically presented in 10^x atoms per cubic centimeter, where x is from 13 to 20 and is typically in the high teens (applicant is

not aware of a practice in this art that refers to impurity concentration in atoms per cubic meter). Copies of graphs from several texts are enclosed showing that the conventional practice is to refer to impurity concentrations in atoms per cubic centimeter where the power of ten is in the range of 10^{13} - 10^{20} . If atoms per cubic meter were being used, the power of ten would be 10^6 times higher (i.e., power of ten would be 10^{19} - 10^{26} and typically in the mid twenties). One of skill in the art would immediately recognize the difference in the power of ten and know that the present application clearly refers to cubic centimeters. Indeed, one of skill in the art would immediately question the original specification in which the impurity concentration is in cubic meters but the power of ten shown is typical for cubic centimeters and simply understand that reference is being made to atoms per cubic centimeter.

One of skill in the art would also infer that atoms per cubic centimeter are to be used in view of the disclosure that an aspect of the invention is that an active layer with two different dislocation density regions has an impurity concentration less than 1×10^{18} atoms per cubic "meter". This number of atoms would be less than 1×10^{12} atoms per cubic centimeter. This number of atoms is far too low to be meaningful (e.g., see the above mentioned graphs) and one of skill in the art would immediately recognize that 1×10^{18} atoms per cubic centimeter were intended. Thus, the change from cubic meters to

cubic centimeters merely formalizes that which one of skill in the art would already understand.

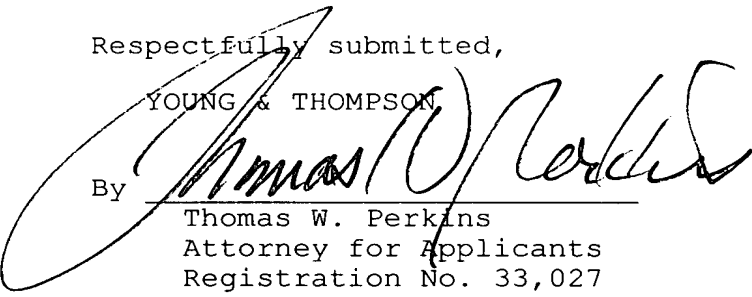
By way of further demonstration that the change merely corrects a typographical error, the present applicant is an inventor in several other pending U.S. patent applications (e.g., see S.N. 09/810,546 at page 5, and S.N. 09/944,186 at page 5), all of which use atoms per cubic centimeter to describe the impurity concentration. This demonstrates that it is the inventor's practice to use cubic centimeters, not cubic meters.

In view of the present amendment and the foregoing remarks, it is believed that the present application has been placed in condition for allowance. Reconsideration and allowance are respectfully requested.

Respectfully submitted,

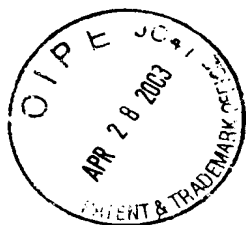
YOUNG & THOMPSON

By



Thomas W. Perkins
Attorney for Applicants
Registration No. 33,027
745 South 23rd Street
Arlington, VA 22202
Telephone: 521-2297

April 28, 2003



5

NITRIDE BASED SEMICONDUCTOR PHOTO-LUMINESCENT DEVICE

BACKGROUND OF THE INVENTION

RECEIVED
10-1-2003
TECHNICAL CENTER 2000

The present invention relates to a nitride based semiconductor
10 device, and more particularly to a nitride based semiconductor
photo-luminescent device.

A nitride based semiconductor is an extremely important material
for a blue-color laser diode. In Jpn. J. Appl. Phys. Vol. 36 (1997), pp.
L1568-1571, Nakamura et al. reported that a continuous
15 photo-luminescence life-time over 10,000 hours at 2 mW output at room
temperature was confirmed. FIG. 1 is a fragmentary cross sectional
elevation view illustrative of a first conventional nitride based
semiconductor laser diode. In order to increase the life-time of the laser
diode, it is essential to reduce the dislocation density of the active layer.
20 The first conventional nitride based semiconductor laser diode has the
following structure. A stripe-shaped silicon dioxide mask 103 having
window regions is selectively formed over a gallium nitride layer 102 over
a top surface of a sapphire substrate 101, so that a gallium nitride layer is
grown over the stripe-shaped silicon dioxide mask 103 and over the

gallium nitride layer 102, wherein the gallium nitride layer has low dislocation density regions 104 which are positioned over the stripe-shaped silicon dioxide mask 103. A p-electrode 105 is positioned over the low dislocation density region 104.

5 A gallium nitride layer 102 is grown on the sapphire substrate 101 by a metal organic chemical vapor deposition method. The sapphire substrate 101 has a high surface dislocation density. The gallium nitride layer 102 has a high dislocation density. A stripe-shaped silicon dioxide mask 103 having window regions is formed over the gallium nitride layer
10 102 in a $[1,-1,0,0]$ -direction. A gallium nitride layer 106 is grown by a metal organic chemical vapor deposition method using the stripe-shaped silicon dioxide mask 103 with the window regions. The gallium nitride layer 106 has a high dislocation density region 116 and a low dislocation density region 104. The high dislocation density region 116 is formed on
15 the gallium nitride layer 102 having a high dislocation density. The high dislocation density region 116 is grown in a vertical direction from gallium nitride layer 102 having a high dislocation density shown by the window regions of the stripe-shaped silicon dioxide mask 103, for which reason the dislocation is propagated from the gallium nitride layer 102 to the high
20 dislocation density region 116, whereby the high dislocation density region 116 has a high dislocation density. The low dislocation density region 104 is formed over the stripe-shaped silicon dioxide mask 103. The low dislocation density region 104 is grown by the epitaxial lateral overgrowth from the window regions of the stripe-shaped silicon dioxide mask 103.

The stripe-shaped silicon dioxide mask 103 cuts the further propagation of the dislocation from the sapphire substrate 101. The low dislocation density region 104 has a low dislocation density. At the center of the low dislocation density region 104, epitaxial lateral overgrowths of gallium nitride in various lateral directions from the window regions of the stripe-shaped silicon dioxide mask 103 come together, whereby new dislocations are formed, for which reason the center region of the low dislocation density region 104 has a high dislocation density. As a result, an Si-doped n-type gallium nitride epitaxial lateral overgrowth substrate 100 is completed which has the high dislocation density region 116 and the low dislocation density region 104.

An Si-doped n-type $\text{In}_{0.1}\text{Ga}_{0.9}\text{N}$ layer 107 is formed over the Si-doped n-type gallium nitride epitaxial lateral overgrowth substrate 100. An n-type cladding layer 108 is formed over the Si-doped n-type $\text{In}_{0.1}\text{Ga}_{0.9}\text{N}$ layer 107, wherein the n-type cladding layer 108 comprises 120 periods of alternating laminations of an Si-doped n-type GaN layer having a thickness of 2.5 nanometers and an undoped $\text{Al}_{0.14}\text{Ga}_{0.86}\text{N}$ layer having a thickness of 2.5 nanometers. An Si-doped n-type GaN optical confinement layer 109 having a thickness of 0.1 micrometers is formed over the n-type cladding layer 108. A multiple quantum well active layer 210 is formed over the Si-doped n-type GaN optical confinement layer 109, wherein the multiple quantum well active layer 210 comprises alternating laminations of Si-doped n-type $\text{In}_{0.15}\text{Ga}_{0.85}\text{N}$ quantum well layer having a thickness of 3.5 nanometers and an Si-doped n-type $\text{In}_{0.02}\text{Ga}_{0.98}\text{N}$

potential barrier layer having a thickness of 10.5 nanometers. An Mg-doped p-type $\text{Al}_{0.2}\text{Ga}_{0.8}\text{N}$ cap layer 111 having a thickness of 20 nanometers is formed over the multiple quantum well active layer 210. An Mg-doped p-type GaN optical confinement layer 112 having a thickness of 5 0.1 micrometer is formed over the Mg-doped p-type $\text{Al}_{0.2}\text{Ga}_{0.8}\text{N}$ cap layer 111. A p-type cladding layer 113 is formed over the Mg-doped p-type GaN optical confinement layer 112, wherein the p-type cladding layer 113 comprises 120 periods of alternating laminations of an Mg-doped p-type GaN layer having a thickness of 2.5 nanometers and an undoped 10 $\text{Al}_{0.14}\text{Ga}_{0.86}\text{N}$ layer having a thickness of 2.5 nanometers. An Mg-doped p-type GaN contact layer 114 having a thickness of 0.05 micrometers is formed over the p-type cladding layer 113. The lamination structure over the Si-doped n-type gallium nitride epitaxial lateral overgrowth substrate 100 is selectively removed by a dry etching process to form a ridge 15 structure over a predetermined region of the top surface of the Si-doped n-type gallium nitride epitaxial lateral overgrowth substrate 100, wherein the ridge structure comprises laminations of the Si-doped n-type $\text{In}_{0.1}\text{Ga}_{0.9}\text{N}$ layer 107, the n-type cladding layer 108, the Si-doped n-type GaN optical confinement layer 109, the multiple quantum well active layer 20 210, the Mg-doped p-type $\text{Al}_{0.2}\text{Ga}_{0.8}\text{N}$ cap layer 111, the Mg-doped p-type GaN optical confinement layer 112, the p-type cladding layer 113 and the Mg-doped p-type GaN contact layer 114. The Mg-doped p-type GaN contact layer 114 is positioned over the low dislocation density region 104 for current injection into the low dislocation density region 104. A

p-electrode 105 is formed on the Mg-doped p-type GaN contact layer 114, wherein the p-electrode 105 comprises an Ni layer and an Au layer. An n-electrode 115 is also selectively formed over the top surface of the Si-doped n-type gallium nitride epitaxial lateral overgrowth substrate 100, wherein the n-electrode 115 comprises an Ni layer and an Au layer. The n-electrode 115 is also positioned over the low dislocation density region 104 for current injection into the low dislocation density region 104.

The gallium nitride substrate formed in the above conventional method is so called to as “epitaxial lateral overgrowth gallium nitride substrate”. The sapphire substrate 101 has a high surface dislocation density. The gallium nitride layer 102 grown over the sapphire substrate 101 also has a high dislocation density. The gallium nitride layer 106 has a high dislocation density region 116 positioned over the window regions of the stripe-shaped silicon dioxide mask 103 and a low dislocation density region 104 positioned over the stripe-shaped silicon dioxide mask 103. The high dislocation density region 116 of the gallium nitride layer 106 was grown over the gallium nitride layer 102 having the high dislocation density, for which reason the high dislocation density region 116 of the gallium nitride layer 106 also has a high dislocation density. The stripe-shaped silicon dioxide mask 103 is made of silicon dioxide free of dislocation, for which reason the low dislocation density region 104 grown over the stripe-shaped silicon dioxide mask 103 has a low dislocation density. The high dislocation density region 116 has a high dislocation density of $1 \times 10^{12} \text{ m}^{-2}$. The stripe-shaped silicon dioxide mask 103 cuts

the propagation of the dislocation from the sapphire substrate 101. The low dislocation density region 104 has a low dislocation density of $1 \times 10^{11} \text{ m}^{-2}$. The low dislocation density region 104 is formed by the epitaxial lateral overgrowth of gallium nitride from the window regions of the stripe-shaped silicon dioxide mask 103. At the center of the low dislocation density region 104, epitaxial lateral overgrowths of gallium nitride in various lateral directions from the window regions of the stripe-shaped silicon dioxide mask 103 come together, whereby new dislocations are formed, for which reason the center region of the low dislocation density region 104 has a high dislocation density. In FIG. 1, the high dislocation density region is represented by dot marks. The p-electrode 105 is formed over the low dislocation density region 104 except for its center region, so that a current is injected from the p-electrode 105 into the low dislocation density region of the active layer. If the current is injected into the high dislocation density region, then the deterioration in performance of the device is likely to appear. However, if the current is injected into the low dislocation density region, then the deterioration in performance of the device is unlikely to appear, resulting in a long life-time of the device.

A second conventional method of forming a low dislocation density region was reported by Nakamura et al. in Applied Physics vol. 68-7, pp. 793-796. A GaN layer is formed on a sapphire substrate. The GaN layer is selectively removed by a dry etching process to form stripe-shaped GaN layers. Further, a GaN layer is formed over the stripe-shaped GaN layers and over the sapphire substrate. The GaN layer is

epitaxially grown in vertical direction from the top surfaces of the stripe-shaped GaN layers and also epitaxially grown by an epitaxial lateral overgrowth in lateral direction from the top surfaces of the stripe-shaped GaN layers toward the top surface of the sapphire substrate. This growth will hereinafter referred to as a “mask-less epitaxial lateral overgrowth”. The GaN layer has a high dislocation density region over the stripe-shaped GaN layer and a low dislocation density region over the sapphire substrate. Namely, the low dislocation density region is grown by the epitaxial lateral overgrowth from the stripe-shaped GaN layers to the region over the uncovered top surface of the sapphire substrate. The stripe-shaped GaN layer has a high dislocation density. The dislocation of the stripe-shaped GaN layer is propagated to the high dislocation density region grown in the vertical direction over the stripe-shaped GaN layers. The dislocation of the stripe-shaped GaN layer is propagated to the low dislocation density region grown by the epitaxial lateral overgrowth from the stripe-shaped GaN layers to the region over the uncovered top surface of the sapphire substrate. A current is injected into the low dislocation density region to obtain a long life-time.

The present inventors reported in Jpn. J. Appl. Phys. Vol. 36 (1997), pp. L899-902 and in NEC Research and Development vol. 41 (2000) No. 1 pp. 74-85 that a low dislocation density region is formed in an entire region of the active layer or an entire region of the substrate by a facet-initiated epitaxial lateral overgrowth method using the stripe-shaped silicon dioxide masks. In accordance with the facet-initiated epitaxial

lateral overgrowth, the stripe-shaped silicon dioxide masks are formed over the gallium nitride layer over the sapphire substrate to carry out a hydride vapor phase epitaxial growth, wherein the through dislocations are curved, whereby the high dislocation density region as the epitaxial lateral
5 overgrowth is not formed. Thus, the dislocation density is suppressed low over the entire of the substrate.

As the technique for forming the low dislocation density GaN region has been progressed, then the life-time of the blue color nitride based semiconductor laser diode, which emits a laser beam of a wavelength
10 in the range of about 400-500 nanometers, has been greatly improved.

The technique for doping silicon into the active layer has been used for improving the laser device performances such as the threshold current density. In Japanese laid-open patent publication No. 10-12969, it is disclosed that silicon impurity is doped into the active layer at an impurity
15 concentration in the range of $1 \times 10^{19} \text{ m}^{-3}$ to $1 \times 10^{21} \text{ cm}^{-3}$ for improvement in the laser threshold value.

In Applied Physics Letter 73 (1998), pp. 496-498 and Proc. of the 2nd Int. Sym. on Blue Laser and Light Emitting Diodes (1998), p. 381, it is disclosed that the active layer is doped with silicon to reduce the
20 threshold value. The mechanism of the threshold value reduction due to the silicon doping process to the active layer might be associated with a piezo electric field shielding effect due to the impurity doping and the improvement in the planarity of the quantum well structure. It has been known that the improvement of the laser device performance is obtainable

by the silicon doping. It is the common technical sense that the advanced nitride based semiconductor laser diode has the active layer which is doped with silicon in the above technical viewpoint.

5 In view of the actual practical use of the laser diode, the reliability of the conventional nitride based semiconductor laser diode is still insufficient. If the nitride based semiconductor laser diode having a wavelength band of about 400-500 nanometers is used for emitting a laser beam for an optical disk such as a digital video disk, a long life-time of not less than 5000 hours at 30 mW and at 70°C is necessary in consideration of
10 the wiring operation. As reported by Nakamura et al. in JSAP International No. 1, pp. 5-17 (2000), the life-time of the conventional nitride based semiconductor laser diodes is only 500 hours at 30 mW and at 60°C.

In the above circumstances, it had been required to develop a novel nitride based semiconductor photo-luminescent device free from the
15 above problem.

SUMMARY OF THE INVENTION

Accordingly, it is an object of the present invention to provide a
20 novel nitride based semiconductor photo-luminescent device free from the above problems.

It is a further object of the present invention to provide a novel nitride based semiconductor photo-luminescent device having a long life-time under high temperature and high output conditions.

The present invention provides a nitride based semiconductor photo-luminescent device having an active layer having a quantum well structure, the active layer having both at least a high dislocation density region and at least a low dislocation density region lower in dislocation
5 density than the high dislocation density region, wherein the low dislocation density region includes a current injection region into which a current is injected, and the active layer is less than $1 \times 10^{18} \text{ cm}^{-3}$ in impurity concentration.

The above and other objects, features and advantages of the
10 present invention will be apparent from the following descriptions.

BRIEF DESCRIPTION OF THE DRAWINGS

Preferred embodiments according to the present invention will be
15 described in detail with reference to the accompanying drawings.

FIG. 1 is a fragmentary cross sectional elevation view illustrative of a first conventional nitride based semiconductor laser diode.

FIG. 2 is a fragmentary cross sectional elevation view illustrative of a first novel nitride based semiconductor laser diode in a first
20 embodiment according to the present invention.

FIG. 3 is a fragmentary cross sectional elevation view illustrative of a second novel nitride based semiconductor laser diode in a second embodiment according to the present invention.

FIG. 4 is a fragmentary cross sectional elevation view illustrative

of a third novel nitride based semiconductor laser diode in a third embodiment according to the present invention.

DISCLOSURE OF THE INVENTION

5

The present inventors found out the extremely important and unexpected facts that if the active layer [is undoped] of the nitride based semiconductor laser device formed over the facet-initiated epitaxial lateral overgrowth gallium nitride substrate is undoped, then a low threshold value
10 is obtained and a longer life-time is also obtained.

The present inventors investigated inter-relationships of the dislocation density distribution, the impurity concentration profile of the active layer, the threshold value of the laser device and the device life-time, wherein the laser diodes are concurrently formed over both different type
15 substrates, for example, the facet-initiated epitaxial lateral overgrowth substrate and the epitaxial lateral overgrowth substrate to prepare the first type semiconductor photo-luminescent devices over the facet-initiated epitaxial lateral overgrowth substrates and also prepare the second type semiconductor photo-luminescent devices over the epitaxial lateral
20 overgrowth substrate. Furthermore, the first type semiconductor photo-luminescent devices over the facet-initiated epitaxial lateral overgrowth substrates may be classified into three different types in Si-impurity concentration in the quantum well active layer.

The first semiconductor photo-luminescent device is formed over

the facet-initiated epitaxial lateral overgrowth substrate and has the Si-undoped quantum well active layer. The second semiconductor photo-luminescent device is formed over the facet-initiated epitaxial lateral overgrowth substrate and has the Si-doped quantum well active layer having a low Si-impurity concentration of $1 \times 10^{18} \text{ cm}^{-3}$. The third semiconductor photo-luminescent device is formed over the facet-initiated epitaxial lateral overgrowth substrate and has the Si-doped quantum well active layer having a high Si-impurity concentration of $5 \times 10^{18} \text{ cm}^{-3}$. The fourth semiconductor photo-luminescent device is formed over the epitaxial lateral overgrowth substrate and has the Si-undoped quantum well active layer. The fifth semiconductor photo-luminescent device is formed over the epitaxial lateral overgrowth substrate and has the Si-doped quantum well active layer having a low Si-impurity concentration of $1 \times 10^{18} \text{ cm}^{-3}$. The sixth semiconductor photo-luminescent device is formed over the epitaxial lateral overgrowth substrate and has the Si-doped quantum well active layer having a high Si-impurity concentration of $5 \times 10^{18} \text{ cm}^{-3}$.

The above first to sixth semiconductor photo-luminescent devices have the same structure as what will be described below in the first embodiment. For the epitaxial lateral overgrowth substrate, a silicon diode mask pattern is used which has a mask width of 20 micrometers and a window of 5 micrometers. This silicon dioxide mask pattern is much wider than the usual silicon dioxide mask pattern having a mask width of not more than about 10 micrometers for the epitaxial lateral overgrowth

substrate. If the mask width is wide, then the wide silicon dioxide mask is buried with the gallium nitride layer by the lateral growth. This makes it difficult to obtain a highly plane layer over the wide silicon dioxide mask. This allows formation of a large low dislocation density region. In accordance with the present invention, a growth condition, for example, a flow rate ratio of Group III element source material and Group V element source material is optimized for forming a planer burying gallium nitride layer grown by the lateral growth over the wide silicon dioxide mask.

Table 1 shows averaged values of individual initial threshold current densities of the above first to sixth nitride based semiconductor laser emitting devices and the degrees of individual deteriorations of the above first to sixth nitride based semiconductor laser emitting devices after APC examination for 100 hours under high temperature and high output conditions of 70°C and 30 mW.

Table 1

	Threshold current density	deterioration
First device	20 (mA/m ²)	no deterioration
Second device	22 (mA/m ²)	no deterioration
Third device	24 (mA/m ²)	no deterioration
Fourth device	23 (mA/m ²)	no deterioration
Fifth device	24 (mA/m ²)	no deterioration
Sixth device	23 (mA/m ²)	slight voltage rise

Threshold current density : initial threshold current density.

The first device : facet-initiated epitaxial lateral overgrowth ; and
Si-undoped quantum well active layer.

The second device : facet-initiated epitaxial lateral overgrowth ; and
Si-doped quantum well active layer of $1 \times 10^{18} \text{ cm}^{-3}$.

5 The third device : facet-initiated epitaxial lateral overgrowth ; and
Si-doped quantum well active layer of $5 \times 10^{18} \text{ cm}^{-3}$.

The fourth device : epitaxial lateral overgrowth ; and
Si-undoped quantum well active layer.

10 The fifth device : epitaxial lateral overgrowth ; and
Si-doped quantum well active layer of $1 \times 10^{18} \text{ cm}^{-3}$.

The sixth device : epitaxial lateral overgrowth ; and
Si-doped quantum well active layer of $5 \times 10^{18} \text{ cm}^{-3}$.

There is no large difference in the initial threshold current density
15 in the first to sixth nitride-based semiconductor laser emitting devices. In
the first and second nitride-based semiconductor laser emitting devices
grown over the facet-initiated epitaxial lateral overgrowth substrates and
having the Si-undoped active layer and the Si-doped active layer of $1 \times$
 10^{18} cm^{-3} , the initial threshold current densities are slightly lower than the
20 remaining initial threshold current densities of the third to sixth
nitride-based semiconductor laser emitting devices, even the Si-impurity
concentrations are lower than $1 \times 10^{19} \text{ cm}^{-3}$. This means that the initial
threshold current density has no large dependency upon the Si-impurity
concentration. In the first to third nitride-based semiconductor laser

emitting devices grown over the facet-initiated epitaxial lateral overgrowth substrates, the first nitride-based semiconductor laser emitting device has the lowest initial threshold current density, and the second nitride-based semiconductor laser emitting device has the second lowest initial threshold current density. If the nitride-based semiconductor laser emitting devices are grown over the facet-initiated epitaxial lateral overgrowth substrates, then the Si-undoped active layer obtains the lowest initial threshold current density. Further, the first to third nitride-based semiconductor laser emitting devices grown over the facet-initiated epitaxial lateral overgrowth substrates are free from any deterioration in performance. The fourth and fifth nitride-based semiconductor laser emitting devices grown over the epitaxial lateral overgrowth substrates and having the Si-undoped active layer and the Si-doped active layer of $1 \times 10^{18} \text{ cm}^{-3}$ are also free from any deterioration in performance. Only the sixth nitride-based semiconductor laser emitting device grown over the epitaxial lateral overgrowth substrate and having the Si-doped active layer of $5 \times 10^{18} \text{ cm}^{-3}$ shows a slight deterioration, for example, a slight voltage raise.

The above experimental results show that the deterioration of the device in the high temperature and high output operation relates to both the presence of the high dislocation density region and the Si-impurity concentration. If the low dislocation density region is entirely grown over the substrate by the facet-initiated epitaxial lateral overgrowth, then the deterioration is unlikely to appear. If not only the low dislocation density region but also the high dislocation density region are grown over the

substrate by the epitaxial lateral overgrowth and if the current is injected into the low dislocation density region, then the deterioration is likely to appear. If not only the low dislocation density region but also the high dislocation density region are grown over the substrate by the epitaxial lateral overgrowth and if the impurity concentration of the active layer is small, then the deterioration is unlikely to appear.

Those mechanisms might be considered as follows. Under the high temperature and high output conditions, a large current flows through the device and a large heat generation is also caused, and further an intensity of the photo-luminescence is high. The heat energy and the energy of photons causes that the dislocations in non-current region outside the active layer extend to the active region, through which a current flows. Once the high dislocation density region reaches the active region, then the deterioration is likely to appear. Doping impurity into the active layer provides an influence to the extension of the dislocations. The impurity introduction causes the local strain in the crystal, thereby making the dislocation further extend and move, and further thereby causes that the photon is absorbed into the impurity level to generate a heat which promotes the extension and motion of the dislocation.

In order to prevent the deteriorations of the device, it is preferable that the entire region of the device is reduced in dislocation density. If the facet-initiated epitaxial lateral overgrowth substrate is used, the low dislocation density region extends entirely over the substrate. It is necessary for forming the facet-initiated epitaxial lateral overgrowth

substrate to prepare not only the metal organic vapor phase epitaxy growth system but also a hydride vapor phase epitaxy growth system. This results in the high manufacturing cost. At the present, the epitaxial lateral overgrowth method and the mask-less epitaxial lateral overgrowth method are advantageous in cost reduction.

If the gallium nitride substrate is prepared by the epitaxial lateral overgrowth method or the mask-less epitaxial lateral overgrowth method, then the following two methods are effective to improve the device life-time under the high temperature and high output conditions. The first method is that the width of the silicon dioxide mask in the epitaxial lateral overgrowth method or the width of the sapphire-exposed region in the mask-less epitaxial lateral overgrowth method is wide to reduce the influence by the high dislocation density region. The second method is that the impurity concentration of the active layer is reduced to suppress the further extension or move of the high dislocation density region to the low dislocation density region.

The above first method needs the large area to be buried by the lateral overgrowth. This means that the growth time necessary for burying the large area by the lateral overgrowth is long, and further makes it difficult to form a plane or flat layer. Notwithstanding, it is possible to bury the flat layer over the large area, for example, the mask width of about 30 micrometers or the sapphire-exposed area of about 30 micrometers under the selected conditions for the lateral overgrowth, for example, the TMG flow rate is not more than 1 micro-mol per 1 minute.

The above second method is opposite to the conventional common sense that doping the silicon impurity reduces the threshold current density. As described above, the present inventors confirmed the fact that the large variation of the threshold current density is independent
5 from the silicon impurity concentration. The experimental results using the facet-initiated epitaxial lateral overgrowth show it is important that the current injection region of the active layer has a low dislocation density and has a reduced number of defects.

The dislocation core causes the non-photo-luminescent
10 re-combination of carriers. In order to suppress the non-photo-luminescent re-combination of carriers, it is effective to increase the impurity concentration of the active layer to shorten the carrier diffusion length thereby suppressing carriers from flowing into the dislocation cores. It has been known that if the impurity concentration is not less than $1 \times 10^{19} \text{ cm}^{-3}$,
15 then Auger re-combination as the non-photo-luminescent re-combination of carriers frequently appears.

In accordance with the conventional common sense, if the dislocation density of the active layer is high, and the impurity concentration is increased to prevent the non-photo-luminescent
20 re-combination at the dislocation cores. The above experimental results show that if the current is injected into the largely reduced dislocation density region, it is more important to reduce the Auger re-combination rather reduce the non-photo-luminescent re-combination at the dislocation cores.

If the active layer comprises a single layered structure of a thickness of not less than 10 nanometers in place of the quantum well structure, the reduction of the Si-impurity concentration into less than $1 \times 10^{18} \text{ cm}^{-3}$ provides a smaller effect for improving the life-time than when
5 the active layer comprises the quantum well structure. If the single layered structure of the active layer has a thickness of less than 10 nanometers, then the quantum effect possessed by the quantum well structure appears, wherein the state density has an abrupt rising edge which increases an optical gain and decreases the threshold current density value, whereby the
10 temperature-dependent characteristics are improved. In this case, the reduction of the Si-impurity concentration into less than $1 \times 10^{18} \text{ cm}^{-3}$ provides a remarkable effect of improving the life-time as in case of the quantum well active layer.

The following is one of the reasons why the effect of improving
15 the life-time is less remarkable if the active layer comprises a thick single layered structure of the thickness of more than 10 nanometers in place of the quantum well structure and if the Si-impurity concentration is less than $1 \times 10^{18} \text{ cm}^{-3}$. The reduction in the Si-impurity concentration of the thick single layered active layer increases the series resistance, whereby the heat
20 generation is increased. The increase in the heat generation causes that even if the Si-impurity concentration is low, then the dislocations are likely to extend and move.

If the active layer comprises the quantum well structure, then the increase in the Si-impurity concentration shortens the life-time. As

compared to the single layered active layer, a ratio in area of the interface to the volume of the active layer is remarkably increased. A segregation of the Si-impurity appears on the interface. Not only the interface recombination speed is increased, but also the extension and move of the
5 dislocations are enhanced.

In accordance with the present invention, the following structures are provided for solving the above issues based on the above technical viewpoint.

The first present invention provides a nitride based
10 semiconductor photo-luminescent device having an active layer having a quantum well structure, the active layer having both at least a high dislocation density region and at least a low dislocation density region lower in dislocation density than the high dislocation density region, wherein the low dislocation density region includes a current injection
15 region into which a current is injected, and the active layer is less than $1 \times 10^{18} \text{ cm}^{-3}$ in impurity concentration.

Since the low dislocation density region includes a current injection region into which a current is injected, and the active layer is less than $1 \times 10^{18} \text{ cm}^{-3}$ in impurity concentration, then the Auger recombination
20 is suppressed and also the extension and move of the high dislocation density region into the current injection region in the low dislocation density region are suppressed, whereby the device life-time under the high temperature and high output conditions is remarkably and greatly improved.

It is preferable that the nitride based semiconductor photo-luminescent device as claimed in claim 1, wherein a dislocation density of the low dislocation density region is not more than one tenth of a dislocation density of the high dislocation density region.

5 It is also preferable that a dislocation density of the current injection region is not more than one tenth of an averaged dislocation density of the active layer.

It is also preferable that a dislocation density of at least a part of the high dislocation density region is not less than $1 \times 10^{12} \text{ m}^{-2}$, and an
10 average dislocation density of the current injection region in the low dislocation density region is less than $1 \times 10^{11} \text{ m}^{-2}$.

It is also preferable that an average dislocation density of the active layer is not less than $1 \times 10^{12} \text{ m}^{-2}$, and an average dislocation density of the current injection region in the low dislocation density region
15 is less than $1 \times 10^{11} \text{ m}^{-2}$.

Since the dislocation density of the current injection region is not more than one tenth of the dislocation density of the high dislocation density region, and further the active layer is less than $1 \times 10^{18} \text{ cm}^{-3}$ in impurity concentration, then the effect is obtained for suppressing the
20 dislocations from the extension and move from the high density dislocation region to the low dislocation density region, particularly into the current injection region.

It is also preferable that an average dislocation density of the current injection region is less than $1 \times 10^{11} \text{ m}^{-2}$, and an average

dislocation density of a peripheral region within a distance of 5 micrometers from the current injection region in the low dislocation density region is not less than $1 \times 10^{12} \text{ m}^{-2}$.

It is also preferable that a current injection electrode is provided
5 over an upper semiconductor layer overlying the active layer, and the active layer has an under-positioned region which is positioned under the current injection electrode, and an average dislocation density of the under-positioned region of the active layer is less than $1 \times 10^{11} \text{ m}^{-2}$, and an average dislocation density of a peripheral region within a distance of 5
10 micrometers from the under-positioned region is not less than $1 \times 10^{12} \text{ m}^{-2}$.

It is also preferable that an average dislocation density of a peripheral region within a distance of 5 micrometers from the current injection region in the low dislocation density region is not more than one tenth of an average dislocation density of the current injection region.

15 It is also preferable that a current injection electrode is provided over an upper semiconductor layer overlying the active layer, and the active layer has an under-positioned region which is positioned under the current injection electrode, and an average dislocation density of the under-positioned region of the active layer is not more than one tenth of an
20 average dislocation density of an average dislocation density of a peripheral region within a distance of 5 micrometers from the under-positioned region.

Since a higher dislocation density region having a dislocation density of not less than ten times of a dislocation density of the current

injection region is present in a peripheral region within a distance of 5 micrometers from the current injection region, and the active layer is less than $1 \times 10^{18} \text{ cm}^{-3}$ in impurity concentration, then the effect is obtained for suppressing the dislocations from the extension and move from the high
5 density dislocation region to the low dislocation density region, particularly into the current injection region.

It is also preferable that the nitride based semiconductor photo-luminescent device is provided over mask patterns provided on a gallium nitride top surface of an epitaxial lateral overgrowth substrate. This
10 structure is advantageous in cost reduction as compared to the facet-initiated epitaxial lateral overgrowth substrate.

It is also preferable that the mask patterns have a mask width of not less than 25 micrometers to increase the width of the low dislocation density region for suppressing the influence by the high dislocation density
15 region and for obtaining the high reliability under the high temperature and high output conditions.

It is also preferable that the nitride based semiconductor photo-luminescent device is provided over selectively provided gallium nitride layers over a semi-insulating substrate of a mask-less epitaxial
20 lateral overgrowth substrate. This structure is advantageous in cost reduction as compared to the facet-initiated epitaxial lateral overgrowth substrate.

It is also preferable that the selectively provided gallium nitride layers have at least a window region having a window width of not less

than 25 micrometers to increase the width of the low dislocation density region for suppressing the influence by the high dislocation density region and for obtaining the high reliability under the high temperature and high output conditions.

5 It is also preferable that the active layer is undoped.

It is also preferable that the active layer comprises a multiple quantum well structure comprising alternating laminations of undoped quantum well layers and undoped potential barrier layers.

It is also preferable that the active layer comprises a multiple
10 quantum well structure comprising alternating laminations of undoped quantum well layers and Si-doped potential barrier layers having an impurity concentration of less than $1 \times 10^{18} \text{ cm}^{-3}$.

It is also preferable that the active layer comprises a multiple quantum well structure comprising alternating laminations of Si-doped
15 quantum well layers having an impurity concentration of less than $1 \times 10^{18} \text{ cm}^{-3}$ and undoped potential barrier layers.

It is also preferable that the active layer comprises a multiple quantum well structure comprising alternating laminations of Si-doped quantum well layers having an impurity concentration of less than 1×10^{18}
20 cm^{-3} and Si-doped potential barrier layers having an impurity concentration of less than $1 \times 10^{18} \text{ cm}^{-3}$.

The second present invention provides a nitride based semiconductor photo-luminescent device having an active layer over an epitaxial lateral overgrowth substrate having a dielectric mask pattern with

a window region, the active layer having both at least a high dislocation density region positioned over the window region and at least a low dislocation density region positioned over the dielectric mask pattern, and the low dislocation density region being lower in dislocation density than
5 the high dislocation density region, wherein the low dislocation density region includes a current injection region into which a current is injected, and the active layer is less than $1 \times 10^{18} \text{ cm}^{-3}$ in impurity concentration.

It is preferable that a dislocation density of the low dislocation density region is not more than one tenth of a dislocation density of the
10 high dislocation density region.

It is also preferable that a dislocation density of the current injection region is not more than one tenth of an averaged dislocation density of the active layer.

It is also preferable that a dislocation density of at least a part of
15 the high dislocation density region is not less than $1 \times 10^{12} \text{ m}^{-2}$, and an average dislocation density of the current injection region in the low dislocation density region is less than $1 \times 10^{11} \text{ m}^{-2}$.

It is also preferable that an average dislocation density of the active layer is not less than $1 \times 10^{12} \text{ m}^{-2}$, and an average dislocation
20 density of the current injection region in the low dislocation density region is less than $1 \times 10^{11} \text{ m}^{-2}$.

It is also preferable that an average dislocation density of the current injection region is less than $1 \times 10^{11} \text{ m}^{-2}$, and an average dislocation density of a peripheral region within a distance of 5

micrometers from the current injection region in the low dislocation density region is not less than $1 \times 10^{12} \text{ m}^{-2}$.

It is also preferable that a current injection electrode is provided over an upper semiconductor layer overlying the active layer, and the active layer has an under-positioned region which is positioned under the current injection electrode, and an average dislocation density of the under-positioned region of the active layer is less than $1 \times 10^{11} \text{ m}^{-2}$, and an average dislocation density of a peripheral region within a distance of 5 micrometers from the under-positioned region is not less than $1 \times 10^{12} \text{ m}^{-2}$.

It is also preferable that an average dislocation density of a peripheral region within a distance of 5 micrometers from the current injection region in the low dislocation density region is not more than one tenth of an average dislocation density of the current injection region.

It is also preferable that a current injection electrode is provided over an upper semiconductor layer overlying the active layer, and the active layer has an under-positioned region which is positioned under the current injection electrode, and an average dislocation density of the under-positioned region of the active layer is not more than one tenth of an average dislocation density of an average dislocation density of a peripheral region within a distance of 5 micrometers from the under-positioned region.

It is also preferable that a higher dislocation density region having a dislocation density of not less than ten times of a dislocation density of the current injection region is present in a peripheral region

within a distance of 5 micrometers from the current injection region.

It is also preferable that the dielectric mask patterns have a mask width of not less than 25 micrometers.

It is also preferable that the dielectric mask patterns comprise
5 single-layered dielectric mask patterns.

It is also preferable that the dielectric mask patterns comprise dielectric multilayer reflective mirrors.

It is also preferable that the active layer is undoped.

It is also preferable that the active layer comprises a multiple
10 quantum well structure comprising alternating laminations of undoped quantum well layers and undoped potential barrier layers.

It is also preferable that the active layer comprises a multiple quantum well structure comprising alternating laminations of undoped quantum well layers and Si-doped potential barrier layers having an
15 impurity concentration of less than $1 \times 10^{18} \text{ cm}^{-3}$.

It is also preferable that the active layer comprises a multiple quantum well structure comprising alternating laminations of Si-doped quantum well layers having an impurity concentration of less than $1 \times 10^{18} \text{ cm}^{-3}$ and undoped potential barrier layers.

20 It is also preferable that the active layer comprises a multiple quantum well structure comprising alternating laminations of Si-doped quantum well layers having an impurity concentration of less than $1 \times 10^{18} \text{ cm}^{-3}$ and Si-doped potential barrier layers having an impurity concentration of less than $1 \times 10^{18} \text{ cm}^{-3}$.

The third present invention provides a nitride based semiconductor photo-luminescent device having an active layer over a mask-less epitaxial lateral overgrowth substrate having a stripe-shaped nitride based semiconductor pattern with a window region, the active layer
5 having both at least a high dislocation density region positioned over the stripe-shaped nitride based semiconductor pattern and at least a low dislocation density region positioned over the window region, and the low dislocation density region being lower in dislocation density than the high dislocation density region, wherein the low dislocation density region
10 includes a current injection region into which a current is injected, and the active layer is less than $1 \times 10^{18} \text{ cm}^{-3}$ in impurity concentration.

It is also preferable that a dislocation density of the low dislocation density region is not more than one tenth of a dislocation density of the high dislocation density region.

15 It is also preferable that a dislocation density of the current injection region is not more than one tenth of an averaged dislocation density of the active layer.

It is also preferable that a dislocation density of at least a part of the high dislocation density region is not less than $1 \times 10^{12} \text{ m}^{-2}$, and an
20 average dislocation density of the current injection region in the low dislocation density region is less than $1 \times 10^{11} \text{ m}^{-2}$.

It is also preferable that an average dislocation density of the active layer is not less than $1 \times 10^{12} \text{ m}^{-2}$, and an average dislocation density of the current injection region in the low dislocation density region

is less than $1 \times 10^{11} \text{ m}^{-2}$.

It is also preferable that an average dislocation density of the current injection region is less than $1 \times 10^{11} \text{ m}^{-2}$, and an average dislocation density of a peripheral region within a distance of 5 micrometers from the current injection region in the low dislocation density region is not less than $1 \times 10^{12} \text{ m}^{-2}$.

It is also preferable that a current injection electrode is provided over an upper semiconductor layer overlying the active layer, and the active layer has an under-positioned region which is positioned under the current injection electrode, and an average dislocation density of the under-positioned region of the active layer is less than $1 \times 10^{11} \text{ m}^{-2}$, and an average dislocation density of a peripheral region within a distance of 5 micrometers from the under-positioned region is not less than $1 \times 10^{12} \text{ m}^{-2}$.

It is also preferable that an average dislocation density of a peripheral region within a distance of 5 micrometers from the current injection region in the low dislocation density region is not more than one tenth of an average dislocation density of the current injection region.

It is also preferable that a current injection electrode is provided over an upper semiconductor layer overlying the active layer, and the active layer has an under-positioned region which is positioned under the current injection electrode, and an average dislocation density of the under-positioned region of the active layer is not more than one tenth of an average dislocation density of an average dislocation density of a peripheral region within a distance of 5 micrometers from the

under-positioned region.

It is also preferable that a higher dislocation density region having a dislocation density of not less than ten times of a dislocation density of the current injection region is present in a peripheral region within a distance of 5 micrometers from the current injection region.

It is also preferable that the window region has a width of not less than 25 micrometers.

It is also preferable that the active layer is undoped.

It is also preferable that the active layer comprises a multiple quantum well structure comprising alternating laminations of undoped quantum well layers and undoped potential barrier layers.

It is also preferable that the active layer comprises a multiple quantum well structure comprising alternating laminations of undoped quantum well layers and Si-doped potential barrier layers having an impurity concentration of less than $1 \times 10^{18} \text{ cm}^{-3}$.

It is also preferable that the active layer comprises a multiple quantum well structure comprising alternating laminations of Si-doped quantum well layers having an impurity concentration of less than $1 \times 10^{18} \text{ cm}^{-3}$ and undoped potential barrier layers.

It is also preferable that the active layer comprises a multiple quantum well structure comprising alternating laminations of Si-doped quantum well layers having an impurity concentration of less than $1 \times 10^{18} \text{ cm}^{-3}$ and Si-doped potential barrier layers having an impurity concentration of less than $1 \times 10^{18} \text{ cm}^{-3}$.

PREFERRED EMBODIMENT

FIRST EMBODIMENT :

5 A first embodiment according to the present invention will be described in detail with reference to the drawings. FIG. 2 is a fragmentary cross sectional elevation view illustrative of a first novel nitride based semiconductor laser diode in a first embodiment according to the present invention. The first novel nitride based semiconductor laser diode has the
10 following structure. A stripe-shaped silicon dioxide mask 103 having window regions is selectively formed over a gallium nitride layer 102 over a top surface of a sapphire substrate 101, so that a gallium nitride layer is grown over the stripe-shaped silicon dioxide mask 103 and over the gallium nitride layer 102, wherein the gallium nitride layer has low
15 dislocation density regions 104 which are positioned over the stripe-shaped silicon dioxide mask 103. Both a first type substrate having a silicon dioxide mask width of 10 micrometers and a second type substrate having a silicon dioxide mask width of 25 micrometers are prepared.

 A gallium nitride layer 102 is grown on the sapphire substrate
20 101 by a metal organic chemical vapor deposition method. The sapphire substrate 101 has a high surface dislocation density. The gallium nitride layer 102 has a high dislocation density. A stripe-shaped silicon dioxide mask 103 having window regions is formed over the gallium nitride layer 102 in a $[1, -1, 0, 0]$ -direction. A gallium nitride layer 106 is grown by a

metal organic chemical vapor deposition method using the stripe-shaped silicon dioxide mask 103 with the window regions. The gallium nitride layer 106 has a high dislocation density region 116 and a low dislocation density region 104. The high dislocation density region 116 is formed on the gallium nitride layer 102 having a high dislocation density. The high dislocation density region 116 is grown in a vertical direction from gallium nitride layer 102 having a high dislocation density shown by the window regions of the stripe-shaped silicon dioxide mask 103, for which reason the dislocation is propagated from the gallium nitride layer 102 to the high dislocation density region 116, whereby the high dislocation density region 116 has a high dislocation density. The low dislocation density region 104 is formed over the stripe-shaped silicon dioxide mask 103. The low dislocation density region 104 is grown by the epitaxial lateral overgrowth from the window regions of the stripe-shaped silicon dioxide mask 103. The stripe-shaped silicon dioxide mask 103 cuts the further propagation of the dislocation from the sapphire substrate 101. The low dislocation density region 104 has a low dislocation density. At the center of the low dislocation density region 104, epitaxial lateral overgrowths of gallium nitride in various lateral directions from the window regions of the stripe-shaped silicon dioxide mask 103 come together, whereby new dislocations are formed, for which reason the center region of the low dislocation density region 104 has a high dislocation density. As a result, an Si-doped n-type gallium nitride epitaxial lateral overgrowth substrate 100 is completed which has the high dislocation density region 116 and the low

dislocation density region 104.

An Si-doped n-type $\text{In}_{0.1}\text{Ga}_{0.9}\text{N}$ layer 107 is formed over the Si-doped n-type gallium nitride epitaxial lateral overgrowth substrate 100. An n-type cladding layer 108 is formed over the Si-doped n-type $\text{In}_{0.1}\text{Ga}_{0.9}\text{N}$ layer 107, wherein the n-type cladding layer 108 comprises 120 periods of alternating laminations of an Si-doped n-type GaN layer having a thickness of 2.5 nanometers and an undoped $\text{Al}_{0.14}\text{Ga}_{0.86}\text{N}$ layer having a thickness of 2.5 nanometers. An Si-doped n-type GaN optical confinement layer 109 having a thickness of 0.1 micrometers is formed over the n-type cladding layer 108. A multiple quantum well active layer 110 is formed over the Si-doped n-type GaN optical confinement layer 109, wherein the multiple quantum well active layer 110 comprises alternating laminations of undoped n-type $\text{In}_{0.15}\text{Ga}_{0.85}\text{N}$ quantum well layer having a thickness of 3.5 nanometers and an undoped n-type $\text{In}_{0.02}\text{Ga}_{0.98}\text{N}$ potential barrier layer having a thickness of 10.5 nanometers. An Mg-doped p-type $\text{Al}_{0.2}\text{Ga}_{0.8}\text{N}$ cap layer 111 having a thickness of 20 nanometers is formed over the multiple quantum well active layer 110. An Mg-doped p-type GaN optical confinement layer 112 having a thickness of 0.1 micrometer is formed over the Mg-doped p-type $\text{Al}_{0.2}\text{Ga}_{0.8}\text{N}$ cap layer 111. A p-type cladding layer 113 is formed over the Mg-doped p-type GaN optical confinement layer 112, wherein the p-type cladding layer 113 comprises 120 periods of alternating laminations of an Mg-doped p-type GaN layer having a thickness of 2.5 nanometers and an undoped $\text{Al}_{0.14}\text{Ga}_{0.86}\text{N}$ layer having a thickness of 2.5 nanometers. An Mg-doped p-type GaN contact

layer 114 having a thickness of 0.05 micrometers is formed over the p-type cladding layer 113. The lamination structure over the Si-doped n-type gallium nitride epitaxial lateral overgrowth substrate 100 is selectively removed by a dry etching process to form a ridge structure over a
5 predetermined region of the top surface of the Si-doped n-type gallium nitride epitaxial lateral overgrowth substrate 100, wherein the ridge structure comprises laminations of the Si-doped n-type $\text{In}_{0.1}\text{Ga}_{0.9}\text{N}$ layer 107, the n-type cladding layer 108, the Si-doped n-type GaN optical confinement layer 109, the undoped multiple quantum well active layer 110,
10 the Mg-doped p-type $\text{Al}_{0.2}\text{Ga}_{0.8}\text{N}$ cap layer 111, the Mg-doped p-type GaN optical confinement layer 112, the p-type cladding layer 113 and the Mg-doped p-type GaN contact layer 114. The Mg-doped p-type GaN contact layer 114 is positioned over the low dislocation density region 104 for current injection into the low dislocation density region 104. A
15 p-electrode 105 is formed on the Mg-doped p-type GaN contact layer 114, wherein the p-electrode 105 comprises an Ni layer and an Au layer. An n-electrode 115 is also selectively formed over the top surface of the Si-doped n-type gallium nitride epitaxial lateral overgrowth substrate 100, wherein the n-electrode 115 comprises an Ni layer and an Au layer. The
20 n-electrode 115 is also positioned over the low dislocation density region 104 for current injection into the low dislocation density region 104.

As compared to the above first and second types novel devices, third to sixth types devices were also prepared. The above first type device has the undoped active region and has the silicon dioxide mask pattern

width of 10 micrometers, wherein the quantum well layers and the potential barrier layers are undoped. The above second type device has the undoped active region and has the silicon dioxide mask pattern width of 25 micrometers. The third to sixth types devices have the Si-doped active layers. The third type device has the silicon dioxide mask pattern width of 10 micrometers and the Si-impurity concentration of $1 \times 10^{18} \text{ cm}^{-3}$ for each of the quantum well layers and the potential barrier layers in the active layer. The fourth type device has the silicon dioxide mask pattern width of 25 micrometers and the Si-impurity concentration of $1 \times 10^{18} \text{ cm}^{-3}$ for each of the quantum well layers and the potential barrier layers in the active layer. The fifth type device has the silicon dioxide mask pattern width of 10 micrometers and the Si-impurity concentration of $5 \times 10^{18} \text{ cm}^{-3}$ for each of the quantum well layers and the potential barrier layers in the active layer. The sixth type device has the silicon dioxide mask pattern width of 25 micrometers and the Si-impurity concentration of $5 \times 10^{18} \text{ cm}^{-3}$ for each of the quantum well layers and the potential barrier layers in the active layer.

Observations to the dislocations for each of the first to sixth types devices have been carried out by use of a transmission electron microscope. The high density dislocation region 116 and the low density dislocation region 104 are observed for each of the first to sixth types devices, wherein the dislocation density of the high dislocation density region 116 is about $5 \times 10^{12} \text{ m}^{-2}$, and the dislocation density of the low dislocation density region 104 is about $2 \times 10^{10} \text{ m}^{-2}$. A large difference in dislocation density was observed between the high dislocation density region 116 and the low

dislocation density region 104. The dislocation density is measurable by the transmission electron microscope. The dislocation density may also be measurable by the etch-pit density. A mixture liquid of phosphoric acid and sulfuric acid is heated at 200°C. Samples of the above six types are dipped
5 into the solution for about 1 hour to form etch-pits at the positions of the dislocations, wherein the etch-pit density almost corresponds to the dislocation density.

If the dislocation density or the etch-pit density is low, then it is necessary for realizing a highly accurate measurement that the number of
10 dislocations or etch-pits distributed in a large area is counted. For example, the dislocation density is about $1 \times 10^{11} \text{ m}^{-2}$, then the area of at least $1 \times 10^{-10} \text{ m}^2$ is necessary for the highly accurate measurement to the dislocation density or the etch-pit density. The area of at least $1 \times 10^{-10} \text{ m}^2$ corresponds to a 10 micrometers squares. If the gallium nitride layer is
15 grown over the epitaxial lateral overgrowth substrate, then the dislocation density has a large special variation in a direction perpendicular to the longitudinal direction of the striped-shape silicon dioxide masks. It is preferable that the measurement is made in a rectangle-shaped area of 100 micrometers in a first direction and 1 micrometer in a second direction,
20 wherein the first direction is parallel to the longitudinal direction of the striped-shape silicon dioxide masks, whilst the second direction is perpendicular to the longitudinal direction of the striped-shape silicon dioxide masks.

Table 2 shows averaged values of individual initial threshold

current densities of the first to sixth samples and the degrees of individual deteriorations thereof after APC examination for 100 hours under high temperature and high output conditions of 70°C and 30 mW.

5

Table 2

	Threshold current density	deterioration
	First sample 22 (mA/m ²)	no deterioration
	Second sample 24 (mA/m ²)	no deterioration
	Third sample 24 (mA/m ²)	no deterioration
10	Fourth sample 23 (mA/m ²)	no deterioration
	Fifth sample 23 (mA/m ²)	emission discontinuation
	Sixth sample 23 (mA/m ²)	no deterioration

Threshold current density : initial threshold current density.

First sample : epitaxial lateral overgrowth ;

15

silicon dioxide mask width of 25 micrometers ; and
Si-undoped active layer.

Second sample : epitaxial lateral overgrowth ;

silicon dioxide mask width of 10 micrometers ; and
Si-undoped active layer.

20

Third sample : epitaxial lateral overgrowth ;

silicon dioxide mask width of 25 micrometers ; and
Si-doped active layer of $1 \times 10^{18} \text{ cm}^{-3}$.

Fourth sample : epitaxial lateral overgrowth ;

silicon dioxide mask width of 10 micrometers ; and

- Si-doped active layer of $1 \times 10^{18} \text{ cm}^{-3}$.
- Fifth sample : epitaxial lateral overgrowth ;
silicon dioxide mask width of 25 micrometers ; and
Si-doped active layer of $5 \times 10^{18} \text{ cm}^{-3}$.
- 5 Sixth sample : epitaxial lateral overgrowth ;
silicon dioxide mask width of 10 micrometers ; and
Si-doped active layer of $5 \times 10^{18} \text{ cm}^{-3}$.

There was no large difference in the initial threshold current
10 density in the above first to sixth samples. The fifth sample having the
mask width of 10 micrometers and the Si-impurity concentration of $5 \times$
 10^{18} cm^{-3} for the active layer showed a remarkable deterioration, wherein
the laser emission is discontinued before 100 hours operation, whilst the
remaining first to fourth and sixth samples showed almost no deteriorations.

15 The fifth sample was observed in dislocation by the transmission electron
microscope. It was confirmed that the dislocations in the high dislocation
density region extend to the low dislocation density region.

Before this examination, the high dislocation density region of
each of the above first to sixth samples was distanced by about 3
20 micrometers from the current injection region of the active layer. After the
examination, the high dislocation density region of the fifth sample only
extends to the current injection region of the active layer. After the
examination, the high dislocation density region of each of the above first
and second samples remained distanced by about 3 micrometers from the

current injection region of the active layer. Namely, the distribution of the dislocation density remained unchanged for the first and second samples having the undoped active layers. For the sixth sample, it was observed that the dislocations extend from the high dislocation density region 116 by
5 about 5 micrometers toward the low dislocation density region 104 but did not reach the current injection region of the active layer.

In accordance with this embodiment, if the high dislocation density region 116 is present within 5 micrometers from the current injection region of the active layer, the low impurity concentration of not
10 more than $1 \times 10^{18} \text{ cm}^{-3}$ of the active layer provides a remarkable effect of suppressing the dislocation motion and extension. If the active layer is undoped or the silicon dioxide mask width is not less than 25 micrometers, then the movement or extension of the dislocation from the high dislocation density region to the low dislocation density region is suppressed, the
15 life-time of the laser device under the high temperature and high output conditions is remarkably and greatly improved.

In order to show the effect of the improved life-time of the device in this embodiment, the comparative samples were prepared, which have various dislocation densities of the high dislocation density region and the
20 low dislocation density regions. The APC examinations were made for each of the comparative samples under the high temperature and high output conditions. The dislocation density is controllable by controlling the growth conditions for the selective growth process.

As a result, in accordance with the present embodiment, even if

the dislocation density of the low dislocation density region is not more than one tenth of the dislocation density of the high dislocation density region. then the Si-undoped active layer results in no deterioration and provides the long life-time in consideration that the dislocation extends or
5 moves from the high dislocation density region to deteriorate the device, if the spatial distribution of the dislocation density, for example, the in-plane variation of the dislocation density is not so large, then the above effect is small and the above result is the natural result. If the dislocation density is uniform spatially, then no further effect of improving the life-time is
10 obtained.

The impurity doping into the active layer means the impurity doping into either any one or both of the quantum well layers and the potential barrier layers. Namely, all of the quantum well layers and the potential barrier layers in the active layer are undoped or Si-doped at an
15 impurity concentration of less than $1 \times 10^{18} \text{ cm}^{-3}$ in order to realize the long-life-time of the device.

In place of the multiple quantum well active layer, the single layered InGaN active layer is used for a further comparative examination. If the thickness of the single layered InGaN active layer is not less than 10
20 nanometers, then the low impurity concentration of less than $1 \times 10^{18} \text{ cm}^{-3}$ provides no remarkable effect of improving the life-time as compared to the multiple quantum well active layer. If the thickness of the single layered InGaN active layer is less than 10 nanometers to form a single quantum well layer for causing quantum effects, then the low impurity concentration

of less than $1 \times 10^{18} \text{ cm}^{-3}$ provides such the remarkable effect of improving the life-time as the multiple quantum well active layer.

The following is one of the reasons why the effect of improving the life-time is less remarkable if the InGaN active layer comprises a thick single layered structure of the thickness of more than 10 nanometers in place of the quantum well structure and if the Si-impurity concentration is less than $1 \times 10^{18} \text{ cm}^{-3}$. The reduction in the Si-impurity concentration of the thick single layered active layer increases the series resistance, whereby the heat generation is increased. The increase in the heat generation causes that even if the Si-impurity concentration is low, then the dislocations are likely to extend and move.

If the active layer comprises the quantum well structure, then the increase in the Si-impurity concentration shortens the life-time. As compared to the single layered active layer, a ratio in area of the interface to the volume of the active layer is remarkably increased. A segregation of the Si-impurity appears on the interface. Not only the interface recombination speed is increased, but also the extension and move of the dislocations are enhanced.

As disclosed in Japanese laid-open patent publication No. 10-12969, other impurity such as Mg than Si is doped to reduce the threshold current density. If the other impurity is not doped into the active layer or the active layer is Mg-undoped, the life-time is largely and greatly improved under the high temperature and high output conditions. The present inventors prepared the different devices having the undoped active

layer and the Mg-doped active layer for carrying out the APC examination at 70°C and 30 mW. The deterioration of the device having the Mg-doped active layer is larger than the deterioration of the device having the undoped active layer.

5 In this embodiment, the novel nitride based semiconductor photo-luminescent device is applied to the semiconductor laser device. It is of course possible to apply the novel nitride based semiconductor photo-luminescent device to other devices such as the light emission diode and the super luminescent diode.

10 In accordance with the novel nitride based semiconductor photo-luminescent device, the active layer has the high dislocation density region and the low dislocation density region which has the current injection layer, and the active layer is less than $1 \times 10^{18} \text{ cm}^{-3}$ in impurity concentration to suppress the Auger re-combination and also suppress the
15 extension and movement of the dislocations from the high dislocation density region to the current injection region in the low dislocation density region, whereby the life-time of the device under the high temperature and high output conditions is remarkably and greatly improved.

20 The nitride based semiconductor photo-luminescent device is formed over the mask patterns provided on the gallium nitride top surface of the epitaxial lateral overgrowth substrate, wherein said mask patterns have a mask width of not less than 25 micrometers to increase the width of the low dislocation density region for suppressing the influence by the high dislocation density region and for obtaining the high reliability under the

high temperature and high output conditions.

SECOND EMBODIMENT :

A second embodiment according to the present invention will be
5 described in detail with reference to the drawings. FIG. 3 is a fragmentary
cross sectional elevation view illustrative of a second novel nitride based
semiconductor laser diode in a second embodiment according to the present
invention. The second novel nitride based semiconductor laser diode is
formed over a mask-less epitaxial lateral overgrowth substrate. a gallium
10 nitride layer 102 is grown over a top surface of a sapphire substrate 101 by
a metal organic chemical vapor deposition. A stripe-shape silicon dioxide
mask 103 is formed over the gallium nitride layer 102, so that the gallium
nitride layer 102 is then selectively etched by a dry etching process to form
a stripe-shaped gallium nitride layer 301 with a window region. The
15 stripe-shape silicon dioxide mask 103 is then removed from the
stripe-shaped gallium nitride layer 301. An Si-doped n-type gallium nitride
layer 302 is grown by the metal organic chemical vapor deposition method
over the stripe-shaped gallium nitride layer 301 with the window region, on
which the top surface of the sapphire substrate 101 is shown, wherein the
20 epitaxial lateral overgrowth appears over the top surface of the sapphire
substrate 101 shown through the window region of the stripe-shaped
gallium nitride layer 301, whilst the normal epitaxial vertical growth
appears over the stripe-shaped gallium nitride layer 301. The epitaxial
lateral overgrowth forms the flat Si-doped n-type gallium nitride layer 302.

The Si-doped n-type gallium nitride layer 302 has a low dislocation density region 104 which is positioned over the window region of the stripe-shaped gallium nitride layer 301. The Si-doped n-type gallium nitride layer 302 has a high dislocation density region 116 which is positioned over the stripe-shaped gallium nitride layer 301.

A gallium nitride layer 102 is grown on the sapphire substrate 101 by a metal organic chemical vapor deposition method. The sapphire substrate 101 has a high surface dislocation density. The gallium nitride layer 102 has a high dislocation density. A stripe-shaped silicon dioxide mask 103 having window regions is formed over the gallium nitride layer 102 in a $[1,-1,0,0]$ -direction for subsequent dry etching to the gallium nitride layer 102 to form a stripe-shaped gallium nitride layer 301 with a window region. The stripe-shape silicon dioxide mask 103 is then removed from the stripe-shaped gallium nitride layer 301. An Si-doped n-type gallium nitride layer 302 is grown by the metal organic chemical vapor deposition method over the stripe-shaped gallium nitride layer 301 with the window region, on which the top surface of the sapphire substrate 101 is shown, wherein the epitaxial lateral overgrowth appears over the top surface of the sapphire substrate 101 shown through the window region of the stripe-shaped gallium nitride layer 301, whilst the normal epitaxial vertical growth appears over the stripe-shaped gallium nitride layer 301. The epitaxial lateral overgrowth forms the flat Si-doped n-type gallium nitride layer 302. The Si-doped n-type gallium nitride layer 302 has a high dislocation density region 116 and a low dislocation density region 104.

The high dislocation density region 116 is formed on the stripe-shaped gallium nitride layer 301 having a high dislocation density. The high dislocation density region 116 is grown in a vertical direction from the stripe-shaped gallium nitride layer 301 having a high dislocation density, for which reason the dislocation is propagated from the stripe-shaped gallium nitride layer 301 to the Si-doped n-type gallium nitride layer 302, whereby the high dislocation density region 116 has a high dislocation density. The low dislocation density region 104 is formed over the top surface of the sapphire substrate 101 shown through the window region of the Si-doped n-type gallium nitride layer 302. The low dislocation density region 104 is grown by the epitaxial lateral overgrowth from the Si-doped n-type gallium nitride layer 302. The interface of the Si-doped n-type gallium nitride layer 302 to the sapphire substrate 101 cuts the further propagation of the dislocation from the sapphire substrate 101. The low dislocation density region 104 has a low dislocation density. At the center of the low dislocation density region 104, epitaxial lateral overgrowths of gallium nitride in various lateral directions from the Si-doped n-type gallium nitride layer 302 come together, whereby new dislocations are formed, for which reason the center region of the low dislocation density region 104 has a high dislocation density. As a result, an Si-doped n-type gallium nitride mask-less epitaxial lateral overgrowth substrate 200 is completed which has the high dislocation density region 116 and the low dislocation density region 104.

Both a first type substrate having a window region width of 10

micrometers and a second type substrate having a window region width of 25 micrometers are prepared.

Further, an Si-doped n-type $\text{In}_{0.1}\text{Ga}_{0.9}\text{N}$ layer 107 is formed over the Si-doped n-type gallium nitride mask-less epitaxial lateral overgrowth substrate 200. An n-type cladding layer 108 is formed over the Si-doped n-type $\text{In}_{0.1}\text{Ga}_{0.9}\text{N}$ layer 107, wherein the n-type cladding layer 108 comprises 120 periods of alternating laminations of an Si-doped n-type GaN layer having a thickness of 2.5 nanometers and an undoped $\text{Al}_{0.14}\text{Ga}_{0.86}\text{N}$ layer having a thickness of 2.5 nanometers. An Si-doped n-type GaN optical confinement layer 109 having a thickness of 0.1 micrometers is formed over the n-type cladding layer 108. A multiple quantum well active layer 110 is formed over the Si-doped n-type GaN optical confinement layer 109, wherein the multiple quantum well active layer 110 comprises alternating laminations of undoped n-type $\text{In}_{0.15}\text{Ga}_{0.85}\text{N}$ quantum well layer having a thickness of 3.5 nanometers and an undoped n-type $\text{In}_{0.02}\text{Ga}_{0.98}\text{N}$ potential barrier layer having a thickness of 10.5 nanometers. An Mg-doped p-type $\text{Al}_{0.2}\text{Ga}_{0.8}\text{N}$ cap layer 111 having a thickness of 20 nanometers is formed over the multiple quantum well active layer 110. An Mg-doped p-type GaN optical confinement layer 112 having a thickness of 0.1 micrometer is formed over the Mg-doped p-type $\text{Al}_{0.2}\text{Ga}_{0.8}\text{N}$ cap layer 111. A p-type cladding layer 113 is formed over the Mg-doped p-type GaN optical confinement layer 112, wherein the p-type cladding layer 113 comprises 120 periods of alternating laminations of an Mg-doped p-type GaN layer having a

thickness of 2.5 nanometers and an undoped $\text{Al}_{0.14}\text{Ga}_{0.86}\text{N}$ layer having a thickness of 2.5 nanometers. An Mg-doped p-type GaN contact layer 114 having a thickness of 0.05 micrometers is formed over the p-type cladding layer 113. The lamination structure over the Si-doped n-type gallium nitride mask-less epitaxial lateral overgrowth substrate 200 is selectively removed by a dry etching process to form a ridge structure over a predetermined region of the top surface of the Si-doped n-type gallium nitride mask-less epitaxial lateral overgrowth substrate 200, wherein the ridge structure comprises laminations of the Si-doped n-type $\text{In}_{0.1}\text{Ga}_{0.9}\text{N}$ layer 107, the n-type cladding layer 108, the Si-doped n-type GaN optical confinement layer 109, the undoped multiple quantum well active layer 110, the Mg-doped p-type $\text{Al}_{0.2}\text{Ga}_{0.8}\text{N}$ cap layer 111, the Mg-doped p-type GaN optical confinement layer 112, the p-type cladding layer 113 and the Mg-doped p-type GaN contact layer 114. The Mg-doped p-type GaN contact layer 114 is positioned over the low dislocation density region 104 for current injection into the low dislocation density region 104. A p-electrode 105 is formed on the Mg-doped p-type GaN contact layer 114, wherein the p-electrode 105 comprises an Ni layer and an Au layer. An n-electrode 115 is also selectively formed over the top surface of the Si-doped n-type gallium nitride mask-less epitaxial lateral overgrowth substrate 200, wherein the n-electrode 115 comprises an Ni layer and an Au layer. The n-electrode 115 is also positioned over the low dislocation density region 104 for current injection into the low dislocation density region 104.

As compared to the above first and second types novel devices, third to sixth types devices were also prepared. The above first type device has the undoped active region and has the window region width of 10 micrometers, wherein the quantum well layers and the potential barrier layers are undoped. The above second type device has the undoped active region and has the window region width of 25 micrometers. The third to sixth types devices have the Si-doped active layers. The third type device has the window region width of 10 micrometers and the Si-impurity concentration of $1 \times 10^{18} \text{ cm}^{-3}$ for each of the quantum well layers and the potential barrier layers in the active layer. The fourth type device has the window region width of 25 micrometers and the Si-impurity concentration of $1 \times 10^{18} \text{ cm}^{-3}$ for each of the quantum well layers and the potential barrier layers in the active layer. The fifth type device has the window region width of 10 micrometers and the Si-impurity concentration of $5 \times 10^{18} \text{ cm}^{-3}$ for each of the quantum well layers and the potential barrier layers in the active layer. The sixth type device has the window region width of 25 micrometers and the Si-impurity concentration of $5 \times 10^{18} \text{ cm}^{-3}$ for each of the quantum well layers and the potential barrier layers in the active layer.

Observations to the dislocations for each of the first to sixth types devices have been carried out by use of a transmission electron microscope. The high density dislocation region 116 and the low density dislocation region 104 are observed for each of the first to sixth types devices, wherein the dislocation density of the high dislocation density region 116 is about 5

$\times 10^{12} \text{ m}^{-2}$, and the dislocation density of the low dislocation density region 104 is about $2 \times 10^{10} \text{ m}^{-2}$. A large difference in dislocation density was observed between the high dislocation density region 116 and the low dislocation density region 104. The dislocation density is measurable by the transmission electron microscope. The dislocation density may also be measurable by the etch-pit density. A mixture liquid of phosphoric acid and sulfuric acid is heated at 200°C . Samples of the above six types are dipped into the solution for about 1 hour to form etch-pits at the positions of the dislocations, wherein the etch-pit density almost corresponds to the dislocation density.

If the dislocation density or the etch-pit density is low, then it is necessary for realizing a highly accurate measurement that the number of dislocations or etch-pits distributed in a large area is counted. For example, the dislocation density is about $1 \times 10^{11} \text{ m}^{-2}$, then the area of at least $1 \times 10^{-10} \text{ m}^2$ is necessary for the highly accurate measurement to the dislocation density or the etch-pit density. The area of at least $1 \times 10^{-10} \text{ m}^2$ corresponds to a 10 micrometers squares. If the gallium nitride layer is grown over the epitaxial lateral overgrowth substrate, then the dislocation density has a large special variation in a direction perpendicular to the longitudinal direction of the striped-shape silicon dioxide masks. It is preferable that the measurement is made in a rectangle-shaped area of 100 micrometers in a first direction and 1 micrometer in a second direction, wherein the first direction is parallel to the longitudinal direction of the striped-shape silicon dioxide masks, whilst the second direction is

perpendicular to the longitudinal direction of the striped-shape silicon dioxide masks.

Table 3 shows averaged values of individual initial threshold current densities of the first to sixth samples and the degrees of individual deteriorations thereof after APC examination for 100 hours under high temperature and high output conditions of 70°C and 30 mW.

Table 3

	Threshold current density	deterioration
10	First sample 24 (mA/m ²)	no deterioration
	Second sample 23 (mA/m ²)	no deterioration
	Third sample 22 (mA/m ²)	no deterioration
	Fourth sample 24 (mA/m ²)	no deterioration
	Fifth sample 22 (mA/m ²)	emission discontinuation
15	Sixth sample 23 (mA/m ²)	no deterioration

Threshold current density : initial threshold current density.

First sample : mask-less epitaxial lateral overgrowth ;
silicon dioxide mask width of 25 micrometers ; and
Si-undoped active layer.

20 Second sample : mask-less epitaxial lateral overgrowth ;
silicon dioxide mask width of 10 micrometers ; and
Si-undoped active layer.

Third sample : mask-less epitaxial lateral overgrowth ;
silicon dioxide mask width of 25 micrometers ; and

- Si-doped active layer of $1 \times 10^{18} \text{ cm}^{-3}$.
- Fourth sample : mask-less epitaxial lateral overgrowth ;
silicon dioxide mask width of 10 micrometers ; and
Si-doped active layer of $1 \times 10^{18} \text{ cm}^{-3}$.
- 5 Fifth sample : mask-less epitaxial lateral overgrowth ;
silicon dioxide mask width of 25 micrometers ; and
Si-doped active layer of $5 \times 10^{18} \text{ cm}^{-3}$.
- Sixth sample : mask-less epitaxial lateral overgrowth ;
silicon dioxide mask width of 10 micrometers ; and
10 Si-doped active layer of $5 \times 10^{18} \text{ cm}^{-3}$.

There was no large difference in the initial threshold current density in the above first to sixth samples. The fifth sample having the mask width of 10 micrometers and the Si-impurity concentration of $5 \times$
15 10^{18} cm^{-3} for the active layer showed a remarkable deterioration, wherein the laser emission is discontinued before 100 hours operation, whilst the remaining first to fourth and sixth samples showed almost no deteriorations. The fifth sample was observed in dislocation by the transmission electron microscope. It was confirmed that the dislocations in the high dislocation
20 density region extend to the low dislocation density region.

Before this examination, the high dislocation density region of each of the above first to sixth samples was distanced by about 3 micrometers from the current injection region of the active layer. After the examination, the high dislocation density region of the fifth sample only

extends to the current injection region of the active layer. After the examination, the high dislocation density region of each of the above first and second samples remained distanced by about 3 micrometers from the current injection region of the active layer. Namely, the distribution of the dislocation density remained unchanged for the first and second samples having the undoped active layers. For the sixth sample, it was observed that the dislocations extend from the high dislocation density region 116 by about 5 micrometers toward the low dislocation density region 104 but did not reach the current injection region of the active layer.

In accordance with this embodiment, if the high dislocation density region 116 is present within 5 micrometers from the current injection region of the active layer, the low impurity concentration of not more than $1 \times 10^{18} \text{ cm}^{-3}$ of the active layer provides a remarkable effect of suppressing the dislocation motion and extension. If the active layer is undoped or the silicon dioxide mask width is not less than 25 micrometers, then the movement or extension of the dislocation from the high dislocation density region to the low dislocation density region is suppressed, the life-time of the laser device under the high temperature and high output conditions is remarkably and greatly improved.

In order to show the effect of the improved life-time of the device in this embodiment, the comparative samples were prepared, which have various dislocation densities of the high dislocation density region and the low dislocation density regions. The APC examinations were made for each of the comparative samples under the high temperature and high

output conditions. The dislocation density is controllable by controlling the growth conditions for the selective growth process.

As a result, in accordance with the present embodiment, even if the dislocation density of the low dislocation density region is not more than one tenth of the dislocation density of the high dislocation density region, then the Si-undoped active layer results in no deterioration and provides the long life-time in consideration that the dislocation extends or moves from the high dislocation density region to deteriorate the device, if the spatial distribution of the dislocation density, for example, the in-plane variation of the dislocation density is not so large, then the above effect is small and the above result is the natural result. If the dislocation density is uniform spatially, then no further effect of improving the life-time is obtained.

The impurity doping into the active layer means the impurity doping into either any one or both of the quantum well layers and the potential barrier layers. Namely, all of the quantum well layers and the potential barrier layers in the active layer are undoped or Si-doped at an impurity concentration of less than $1 \times 10^{18} \text{ cm}^{-3}$ in order to realize the long-life-time of the device.

In place of the multiple quantum well active layer, the single layered InGaN active layer is used for a further comparative examination. If the thickness of the single layered InGaN active layer is not less than 10 nanometers, then the low impurity concentration of less than $1 \times 10^{18} \text{ cm}^{-3}$ provides no remarkable effect of improving the life-time as compared to

the multiple quantum well active layer. If the thickness of the single layered InGaN active layer is less than 10 nanometers to form a single quantum well layer for causing quantum effects, then the low impurity concentration of less than $1 \times 10^{18} \text{ m}^{-3}$ provides such the remarkable effect of improving the life-time as the multiple quantum well active layer.

The following is one of the reasons why the effect of improving the life-time is less remarkable if the InGaN active layer comprises a thick single layered structure of the thickness of more than 10 nanometers in place of the quantum well structure and if the Si-impurity concentration is less than $1 \times 10^{18} \text{ cm}^{-3}$. The reduction in the Si-impurity concentration of the thick single layered active layer increases the series resistance, whereby the heat generation is increased. The increase in the heat generation causes that even if the Si-impurity concentration is low, then the dislocations are likely to extend and move.

If the active layer comprises the quantum well structure, then the increase in the Si-impurity concentration shortens the life-time. As compared to the single layered active layer, a ratio in area of the interface to the volume of the active layer is remarkably increased. A segregation of the Si-impurity appears on the interface. Not only the interface recombination speed is increased, but also the extension and move of the dislocations are enhanced.

If the other impurity is not doped into the active layer or the active layer is Mg-undoped, the life-time is largely and greatly improved under the high temperature and high output conditions. The present

inventors prepared the different devices having the undoped active layer and the Mg-doped active layer for carrying out the APC examination at 70°C and 30 mW. The deterioration of the device having the Mg-doped active layer is larger than the deterioration of the device having the undoped active layer.

In this embodiment, the novel nitride based semiconductor photo-luminescent device is applied to the semiconductor laser device. It is of course possible to apply the novel nitride based semiconductor photo-luminescent device to other devices such as the light emission diode and the super luminescent diode.

In accordance with the novel nitride based semiconductor photo-luminescent device, the active layer has the high dislocation density region and the low dislocation density region which has the current injection layer, and the active layer is less than $1 \times 10^{18} \text{ cm}^{-3}$ in impurity concentration to suppress the Auger re-combination and also suppress the extension and movement of the dislocations from the high dislocation density region to the current injection region in the low dislocation density region, whereby the life-time of the device under the high temperature and high output conditions is remarkably and greatly improved.

The nitride based semiconductor photo-luminescent device is formed over the mask patterns provided on the gallium nitride top surface of the epitaxial lateral overgrowth substrate, wherein said mask patterns have a mask width of not less than 25 micrometers to increase the width of the low dislocation density region for suppressing the influence by the high

dislocation density region and for obtaining the high reliability under the high temperature and high output conditions.

The nitride based semiconductor photo-luminescent device is formed over selectively provided gallium nitride layers over the
5 semi-insulating substrate of the mask-less epitaxial lateral overgrowth substrate, wherein said selectively provided gallium nitride layers have at least a window region having a window width of not less than 25 micrometers to increase the width of the low dislocation density region for suppressing the influence by the high dislocation density region and for
10 obtaining the high reliability under the high temperature and high output conditions.

THIRD EMBODIMENT :

A third embodiment according to the present invention will be
15 described in detail with reference to the drawings. FIG. 4 is a fragmentary cross sectional elevation view illustrative of a third novel nitride based semiconductor laser diode in a third embodiment according to the present invention. The third novel nitride based semiconductor laser diode comprises a surface emitting laser diode with the following structure. A
20 stripe-shaped multilayer mask 403 having window regions is selectively formed over a gallium nitride layer 102 over a top surface of a sapphire substrate 101, wherein the stripe-shaped multilayer mask 403 comprises 20 periods of alternating laminations of zirconium dioxide film and silicon dioxide film. The stripe-shaped multilayer mask 403 serves as a bottom

dielectric multilayer reflective mirror. A gallium nitride layer 106 is grown over the stripe-shaped multilayer mask 403 and over the gallium nitride layer 102, wherein the gallium nitride layer has low dislocation density regions 104 which are positioned over the stripe-shaped multilayer mask
5 403.

A gallium nitride layer 102 is grown on the sapphire substrate 101 by a metal organic chemical vapor deposition method. The sapphire substrate 101 has a high surface dislocation density. The gallium nitride layer 102 has a high dislocation density. A stripe-shaped multilayer mask
10 403 having window regions is formed over the gallium nitride layer 102 in a $[1,-1,0,0]$ -direction over a top surface of a sapphire substrate 101. A gallium nitride layer 106 is grown by a metal organic chemical vapor deposition method using the stripe-shaped multilayer mask 403 with the window regions. The gallium nitride layer 106 has a high dislocation
15 density region 116 and a low dislocation density region 104. The high dislocation density region 116 is formed on the gallium nitride layer 102 having a high dislocation density. The high dislocation density region 116 is grown in a vertical direction from gallium nitride layer 102 having a high dislocation density shown by the window regions of the stripe-shaped
20 multilayer mask 403, for which reason the dislocation is propagated from the gallium nitride layer 102 to the high dislocation density region 116, whereby the high dislocation density region 116 has a high dislocation density. The low dislocation density region 104 is formed over the stripe-shaped multilayer mask 403. The low dislocation density region 104

is grown by the epitaxial lateral overgrowth from the window regions of the stripe-shaped multilayer mask 403. The stripe-shaped multilayer mask 403 cuts the further propagation of the dislocation from the sapphire substrate 101. The low dislocation density region 104 has a low dislocation density.

5 At the center of the low dislocation density region 104, epitaxial lateral overgrowths of gallium nitride in various lateral directions from the window regions of the stripe-shaped multilayer mask 403 come together, whereby new dislocations are formed, for which reason the center region of the low dislocation density region 104 has a high dislocation density. As a

10 result, an Si-doped n-type gallium nitride epitaxial lateral overgrowth substrate 100 is completed which has the high dislocation density region 116 and the low dislocation density region 104.

A multiple quantum well active layer 110 is formed over the Si-doped n-type gallium nitride epitaxial lateral overgrowth substrate 100,

15 wherein the multiple quantum well active layer 110 comprises alternating laminations of undoped n-type $\text{In}_{0.15}\text{Ga}_{0.85}\text{N}$ quantum well layer having a thickness of 3.5 nanometers and an undoped n-type $\text{In}_{0.02}\text{Ga}_{0.98}\text{N}$ potential barrier layer having a thickness of 10.5 nanometers. An Mg-doped p-type multilayer reflective mirror 413 is formed over the multiple quantum well

20 active layer 110, wherein the Mg-doped p-type multilayer reflective mirror 413 comprises 40 periods of alternating laminations of an Mg-doped p-type $\text{Al}_{0.4}\text{Ga}_{0.6}\text{N}$ layer and an Mg-doped p-type GaN layer. An Mg-doped p-type GaN contact layer 114 having a thickness of 0.05 micrometers is formed over the Mg-doped p-type multilayer reflective mirror 413. The

lamination structure over the Si-doped n-type gallium nitride epitaxial lateral overgrowth substrate 100 is selectively removed by a dry etching process to form a ridge structure over a predetermined region of the top surface of the Si-doped n-type gallium nitride epitaxial lateral overgrowth substrate 100, wherein the ridge structure comprises laminations of the upper region of the gallium nitride layer 106, the undoped multiple quantum well active layer 110, the Mg-doped p-type multilayer reflective mirror 413, and the the Mg-doped p-type GaN contact layer 114. The Mg-doped p-type GaN contact layer 114 is positioned over the low dislocation density region 104 for current injection into the low dislocation density region 104. A p-electrode 105 is formed on the Mg-doped p-type GaN contact layer 114, wherein the p-electrode 105 comprises an Ni layer and an Au layer. An n-electrode 115 is also selectively formed over the top surface of the Si-doped n-type gallium nitride epitaxial lateral overgrowth substrate 100, wherein the n-electrode 115 comprises an Ni layer and an Au layer. The n-electrode 115 is also positioned over the low dislocation density region 104 for current injection into the low dislocation density region 104. A laser is emitted from a bottom surface of the sapphire substrate 101 in a direction vertical to the bottom surface.

As compared to the above first type device, the second and third types devices were also prepared. The above first type device has the undoped active region, wherein the quantum well layers and the potential barrier layers are undoped. The second type device has the Si-doped active region with the Si-impurity concentration of $1 \times 10^{18} \text{ cm}^{-3}$ for each of the

quantum well layers and the potential barrier layers. The second type device has the Si-doped active region with the Si-impurity concentration of $5 \times 10^{18} \text{ cm}^{-3}$ for each of the quantum well layers and the potential barrier layers.

5 Observations to the dislocations for each of the first to third types devices have been carried out by use of a transmission electron microscope. The high density dislocation region 116 and the low density dislocation region 104 are observed for each of the first to third types devices, wherein the dislocation density of the high dislocation density region 116 is about 5
10 $\times 10^{12} \text{ m}^{-2}$, and the dislocation density of the low dislocation density region 104 is about $2 \times 10^{10} \text{ m}^{-2}$. A large difference in dislocation density was observed between the high dislocation density region 116 and the low dislocation density region 104. The dislocation density is measurable by the transmission electron microscope. The dislocation density may also be
15 measurable by the etch-pit density. A mixture liquid of phosphoric acid and sulfuric acid is heated at 200°C . Samples of the above six types are dipped into the solution for about 1 hour to form etch-pits at the positions of the dislocations, wherein the etch-pit density almost corresponds to the dislocation density.

20 If the dislocation density or the etch-pit density is low, then it is necessary for realizing a highly accurate measurement that the number of dislocations or etch-pits distributed in a large area is counted. For example, the dislocation density is about $1 \times 10^{11} \text{ m}^{-2}$, then the area of at least $1 \times 10^{-10} \text{ m}^2$ is necessary for the highly accurate measurement to the

dislocation density or the etch-pit density. The area of at least $1 \times 10^{-10} \text{ m}^2$ corresponds to a 10 micrometers squares. If the gallium nitride layer is grown over the epitaxial lateral overgrowth substrate, then the dislocation density has a large special variation in a direction perpendicular to the longitudinal direction of the striped-shape silicon dioxide masks. It is preferable that the measurement is made in a rectangle-shaped area of 100 micrometers in a first direction and 1 micrometer in a second direction, wherein the first direction is parallel to the longitudinal direction of the striped-shape silicon dioxide masks, whilst the second direction is perpendicular to the longitudinal direction of the striped-shape silicon dioxide masks.

The APC examination for 100 hours under high temperature and high output conditions of 70°C and 30 mW was carried out to the first to third type devices.

There was no large difference in the initial threshold current density in the above first to third devices. The third type device having the Si-impurity concentration of $5 \times 10^{18} \text{ cm}^{-3}$ for the active layer showed a remarkable deterioration, wherein the laser emission is discontinued before 100 hours operation, whilst the remaining first and second type devices showed almost no deteriorations. The third type device was observed in dislocation by the transmission electron microscope. It was confirmed that the dislocations in the high dislocation density region extend to the low dislocation density region.

Before this examination, the high dislocation density region of

each of the above first to third type devices was distanced by about 3 micrometers from the current injection region of the active layer. After the examination, the high dislocation density region of the third type device only extends to the current injection region of the active layer. After the examination, the high dislocation density region of each of the above first and second type devices remained distanced by about 3 micrometers from the current injection region of the active layer. Namely, the distribution of the dislocation density remained unchanged for the first and second type devices having the undoped active layers and the Si-impurity concentration of $5 \times 10^{18} \text{ cm}^{-3}$.

In accordance with this embodiment, if the high dislocation density region 116 is present within 5 micrometers from the current injection region of the active layer, the low impurity concentration of not more than $1 \times 10^{18} \text{ cm}^{-3}$ of the active layer provides a remarkable effect of suppressing the dislocation motion and extension. If the active layer is undoped, then the movement or extension of the dislocation from the high dislocation density region to the low dislocation density region is suppressed, the life-time of the laser device under the high temperature and high output conditions is remarkably and greatly improved.

If the other impurity is not doped into the active layer or the active layer is Mg-undoped, the life-time is largely and greatly improved under the high temperature and high output conditions. The present inventors prepared the different devices having the undoped active layer and the Mg-doped active layer for carrying out the APC examination at

70°C and 30 mW. The deterioration of the device having the Mg-doped active layer is larger than the deterioration of the device having the undoped active layer.

In this embodiment, the novel nitride based semiconductor photo-luminescent device is applied to the semiconductor laser device. It is of course possible to apply the novel nitride based semiconductor photo-luminescent device to other devices such as the light emission diode and the super luminescent diode.

In accordance with the novel nitride based semiconductor photo-luminescent device, the active layer has the high dislocation density region and the low dislocation density region which has the current injection layer, and the active layer is less than $1 \times 10^{18} \text{ cm}^{-3}$ in impurity concentration to suppress the Auger re-combination and also suppress the extension and movement of the dislocations from the high dislocation density region to the current injection region in the low dislocation density region, whereby the life-time of the device under the high temperature and high output conditions is remarkably and greatly improved.

The nitride based semiconductor photo-luminescent device is formed over the mask patterns provided on the gallium nitride top surface of the epitaxial lateral overgrowth substrate, wherein said mask patterns have a mask width of not less than 25 micrometers to increase the width of the low dislocation density region for suppressing the influence by the high dislocation density region and for obtaining the high reliability under the high temperature and high output conditions.

Whereas modifications of the present invention will be apparent to a person having ordinary skill in the art, to which the invention pertains, it is to be understood that embodiments as shown and described by way of illustrations are by no means intended to be considered in a limiting sense. Accordingly, it is to be intended to cover by claims all modifications which fall within the spirit and scope of the present invention.

(19) 日本国特許庁 (J P)

(12) 公開特許公報 (A)

(11) 特許出願公開番号

特開平10-12969

(43) 公開日 平成10年(1998) 1月16日

(51) Int.Cl.⁶

識別記号

庁内整理番号

F I

技術表示箇所

H 0 1 S 3/18

H 0 1 S 3/18

H 0 1 L 33/00

H 0 1 L 33/00

C

審査請求 未請求 請求項の致 4 O L (全 8 頁)

(21) 出願番号

特願平8-157812

(22) 出願日

平成8年(1996) 6月19日

(71) 出願人 000226057

日亜化学工業株式会社

徳島県阿南市上中町岡491番地100

(72) 発明者 長濱 慎一

徳島県阿南市上中町岡491番地100 日亜化学工業株式会社内

(72) 発明者 中村 修二

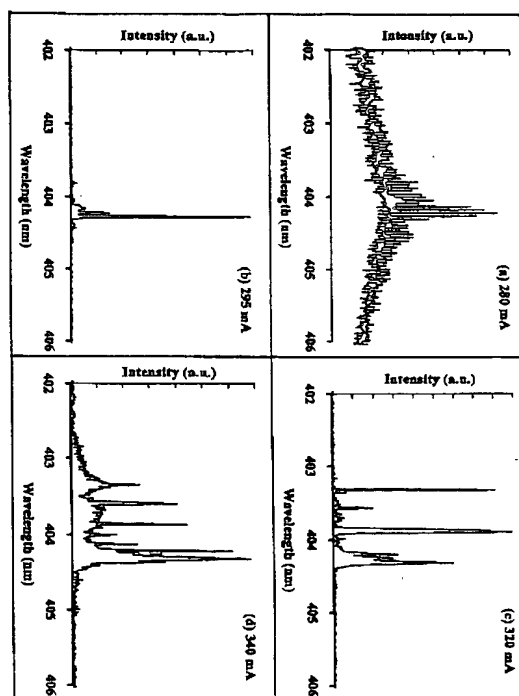
徳島県阿南市上中町岡491番地100 日亜化学工業株式会社内

(54) 【発明の名称】 窒化物半導体レーザ素子

(57) 【要約】

【目的】 窒化物半導体よりなるレーザ素子の発光出力を高め、さらに閾値電流を小さくして、室温での連続発振を目指す。

【構成】 インジウムを含む窒化物半導体よりなる井戸層と、井戸層よりもバンドギャップが大きい窒化物半導体よりなる障壁層とが積層されてなる多重量子井戸構造の活性層を有する窒化物半導体レーザ素子において、前記活性層中にはn型不純物及び／又はp型不純物がドーピングされており、さらに前記レーザ素子の発光スペクトル中には縦モードの発光ピークとは異なる複数の発光ピークを有する。



【特許請求の範囲】

【請求項1】 インジウムを含む窒化物半導体よりなる井戸層と、井戸層よりもバンドギャップが大きい窒化物半導体よりなる障壁層とが積層されてなる多重量子井戸構造の活性層を有する窒化物半導体レーザ素子において、前記活性層中にはn型不純物及び／又はp型不純物がドーピングされており、さらに前記レーザ素子の発光スペクトル中には縦モードの発光ピークとは異なる複数の発光ピークを有することを特徴とする窒化物半導体レーザ素子。

【請求項2】 前記レーザ素子の発光スペクトルの発光ピークが、1 meV～100 meV間隔の範囲内にあることを特徴とする請求項1に記載の窒化物半導体レーザ素子。

【請求項3】 前記活性層にはn型不純物がドーピングされており、 $1 \times 10^{18} / \text{cm}^3 \sim 1 \times 10^{22} / \text{cm}^3$ の濃度でドーピングされていることを特徴とする請求項1または2に記載の窒化物半導体レーザ素子。

【請求項4】 前記活性層にはp型不純物がドーピングされており、 $1 \times 10^{17} / \text{cm}^3 \sim 1 \times 10^{22} / \text{cm}^3$ の濃度でドーピングされていることを特徴とする請求項1乃至3の内のいずれか1項に記載の窒化物半導体レーザ素子。

【発明の詳細な説明】

【0001】

【発明の属する技術分野】本発明は窒化物半導体 ($\text{In}_x\text{Al}_y\text{Ga}_{1-x-y}\text{N}$ 、 $0 \leq x$ 、 $0 \leq y$ 、 $x+y \leq 1$) よりなるレーザ素子に関する。

【0002】

【従来の技術】活性層にSiがドーピングされたレーザ素子が、特開平7-297494号公報に記載されている。この公報にはGa_{0.9}Nよりなる膜厚の厚い活性層にSiをドーピングして閾値電流を低下させることが開示されている。

【0003】しかし、前記公報のように、単一層の膜厚が例えば0.1 μm以上もある厚膜の活性層を有する素子構造では出力が弱く、レーザ発振させるのは非常に困難である。また活性層を単一膜厚が100 Å近辺にある井戸層と障壁層とを積層した多重量子井戸構造の活性層を有するレーザ素子が、例えば特開平8-64909号公報に記載されている。この公報には、井戸層にZnがドーピングされた多重量子井戸構造の活性層を有するレーザ素子が記載されており、井戸層に極微量のZnをドーピングすることにより、価電子帯近くにアクセプター的な不純物準位を形成して、閾値電流を低下させることが示されている。さらにまた、特開平6-268257号公報には $\text{In}_x\text{Ga}_{1-x}\text{N}$ よりなる井戸層と、 $\text{In}_y\text{Ga}_{1-y}\text{N}$ よりなる障壁層とを積層した多重量子井戸構造の活性層を有する発光素子が示されており、さらにこの公報には活性層にn型不純物、またはp型不純物をドーピングしても良いことが記載されている。

【0004】このように活性層にn型、p型不純物をドーピングして、バンドギャップ内に不純物準位を形成することにより、発光素子の発光出力を高めたり、レーザ素子の閾値電流を低下させることが知られている。

【0005】

【発明が解決しようとする課題】ところで、本出願人は最近窒化物半導体により、パルス電流において、室温での410 nmのレーザ発振を発表した(例えば、Jpn.J. Appl. Phys., Vol 35 (1996) pp. L74-76)。発表したレーザ素子はいわゆる電極ストライプ型のレーザ素子であり、ノンドーピングInGa_{0.9}Nが積層された多重量子井戸構造の活性層を有するものである。

【0006】しかしながら、前記窒化物半導体レーザは未だパルス発振でしかなく、しかも閾値電流は1～2 Aもある。窒化物半導体で連続発振させるためには、閾値電流をさらに低下させる必要がある。

【0007】従って、本発明の目的とするところは、窒化物半導体よりなるレーザ素子の発光出力を高め、さらに閾値電流を小さくして、室温での連続発振を目指すことにある。

【0008】

【課題を解決するための手段】本発明のレーザ素子は、インジウムを含む窒化物半導体よりなる井戸層と、井戸層よりもバンドギャップが大きい窒化物半導体よりなる障壁層とが積層されてなる多重量子井戸構造の活性層を有する窒化物半導体レーザ素子において、前記活性層中にはn型不純物及び／又はp型不純物がドーピングされており、さらに前記レーザ素子の発光スペクトル中には縦モードの発光ピークとは異なる複数の発光ピークを有することを特徴とする。

【0009】さらに本発明のレーザ素子は、前記レーザ素子の発光スペクトルの発光ピークは、1 meV～100 meV間隔の範囲内にあることを特徴とする。なお、本発明において、必ずしも隣り合った全ての発光ピークの間隔が前記範囲の間にあることを指すものではない。

【0010】また、活性層にはn型不純物がドーピングされており、そのn型不純物が $1 \times 10^{18} / \text{cm}^3 \sim 1 \times 10^{22} / \text{cm}^3$ の濃度でドーピングされていることが望ましく、さらに好ましくは、n型不純物は少なくとも井戸層にドーピングされていることが望ましい。

【0011】また、活性層にはp型不純物がドーピングされており、そのp型不純物が $1 \times 10^{17} / \text{cm}^3 \sim 1 \times 10^{22} / \text{cm}^3$ の濃度でドーピングされていることが望ましく、さらに好ましくは、p型不純物は少なくとも井戸層にドーピングされていることが望ましい。

【0012】

【発明の実施の形態】図1は本発明の一実施例に係るレーザ素子の構造を示す模式的な断面図である。基本的な構造としては、基板1の上に、バッファ層2、n型コンタクト層3、n型クラッド層4、不純物がドーピングされた

多重量子井戸構造を有する活性層5、第1のp型層6、第2のp型層7、第3のp型層8、p型コンタクト層9が順に積層された電極ストライプ型の構造を有しており、n型コンタクト層にはストライプ状の負電極、p型コンタクト層には正電極が設けられている。

【0013】このレーザ素子を各パルス電流を流した際のスペクトルを図3に示す。図3において(a)は280mA(閾値直後)、(b)は295mA、(c)は320mA、(d)は340mAでの発光スペクトルを示している。(b)、(c)、(d)は発振時のスペクトルを示している。

【0014】(a)は発振直後のスペクトルを示し、この状態ではおよそ404.2nm付近にある主発光ピークの前後に小さな発光ピークが多数(ファブリペローモード)出現してレーザ発振直後の状態であることが分かる。これがいわゆる縦モードのスペクトルである。電流値を上げると(b)に示すように、そのスペクトルがシングルモードとなって404.2nm付近のレーザ発振を示す。次からが本発明の特徴であり、さらに電流を増加させると、(c)に示すように、403.3nm(3.075eV)、403.6nm(3.072eV)、403.9nm(3.070eV)、404.2nm(3.068eV)、404.4nm(3.066eV)というように、主発光ピークの他に、強度の大きな発光ピークが1meV~100meVの間隔で不規則に出現する。さらに(d)では前記ピークの他に、また新たなピークがはっきりと出現しており、これらのスペクトル間隔は一定ではなく明らかに縦モードのスペクトルと異なる。

【0015】一般に、半導体レーザの場合、レーザ発振すると、レーザ光の縦モードによる小さな発光ピークが主発光ピークの前後に多数出現する。この場合の発光スペクトルは、ほぼ等間隔の発光ピークよりなっている。赤色半導体レーザでは、その発光ピークの間隔はおよそ0.2nmである。青色半導体レーザではおよそ0.05nm(1meV)以下である(但し、青色半導体レーザの縦モードは共振器長が600μmにおいて、本出願人により初めて計測された。)。つまり、図3(a)、(b)の状態では通常のレーザ素子の挙動を示している。しかし、本発明のレーザ素子の場合、(c)、(d)に示すように、明らかに従来のレーザ素子の縦モードによる発光ピークとは異なった等間隔でないピークが多数出現している。これは図3の電流値による各スペクトルを比較しても分かる。本発明のレーザ素子では、このような発光スペクトルが出現することにより、出力が高くなる。

【0016】なぜ、このようなピークが発生するとレーザ素子の出力が高くなるのかは定かではないが、例えば次のようなことが考えられる。活性層が量子井戸構造の場合、井戸層の膜厚は100オングストローム以下、好

ましくは70オングストローム以下、最も好ましくは50オングストローム以下に調整される。一方、障壁層も150オングストローム以下、好ましくは100オングストローム以下に調整される。本発明の発光素子では、このような単一膜厚が数十オングストロームの薄膜を積層した場合、井戸層、障壁層共、均一な膜厚で成長しておらず、凹凸のある層が幾重にも重なり合った状態となっている。図2は図1のレーザ素子において活性層5とクラッド層との界面の状態を拡大して示す模式的な断面図である。図2に示すように、このような凹凸のある活性層を、活性層よりもバンドギャップの大きいクラッド層で挟むダブルヘテロ構造を実現すると、活性層に注入された電子とホールとが、凹部にも閉じ込められるようになって、クラッド層の縦方向と共に縦横の両方向に閉じ込められる。このため、キャリアが約10~70オングストローム凹凸差がある3次元のInGa_Nよりなる量子箱、あるいは量子ディスクに閉じ込められたようになって、従来の量子井戸構造とは違った、量子効果出現する。従って、多数の量子準位に基づく発光が室温でも観測されるようになり、発光スペクトルの1meV~100meVの間隔で多数の発光ピークが観測される。また、他の理由としては、三次元のInGa_Nよりなる小さな量子箱にキャリアが閉じ込められるので、エキシトン効果が顕著に現れてきて多数の発光ピークが観測される。

【0017】また、このようにInGa_N井戸層に多数の凹凸が発生する理由の一つとして、In組成の面内不均一が考えられる。即ち、単一井戸層内において、In組成の大きい領域と、少ない領域とができるために、井戸層表面に多数の凹凸が発生するのである。InGa_Nは混晶を成長させにくい材料であり、InNとGa_Nとが相分離する傾向にある。このためIn組成の不均一な領域ができる。そして、このIn組成の高い領域に電子と正孔とが局在して、エキシトン発光、あるいはバイエキシトン発光して、レーザの出力が向上し、多数のピークができる。特にレーザ素子ではこのバイエキシトンレーザ発振することにより、量子ディスク、量子箱と同等になって多数のピークが出現し、この多数のピークによりレーザ素子の閾値が下がり、出力が向上する。なおエキシトンとは電子と正孔とが弱いクーロン力でくっついてペアになったものである。

【0018】さらに、活性層中にn型不純物及び/又はp型不純物をドーピングすることにより、閾値電流を低下させることができる。これらの不純物をドーピングすることにより、活性層のIn組成の多い領域に局在化しているエキシトンが、今度はそれよりもさらに深い不純物の準位に局在化するようになって、エキシトン発光の効果が顕著となることにより、閾値の低下が起きる。

【0019】本発明のレーザ素子の活性層について述べたことを、図6のエネルギーバンド図でわかりやすく示

す。図6Aは多重量子井戸構造の活性層のエネルギーバンドを示しており、図6Bは、図6Aの単一井戸層のエネルギーバンドを拡大して示すものである。前記したように、井戸層においてIn組成の面内不均一があるということは、Bに示すように単一のInGa_N井戸層幅にバンドギャップの異なるInGa_N領域が存在する。従って、伝導帯にある電子は一度、In組成の大きいInGa_N領域に落ちて、そこから価電子帯にある正孔と再結合することによりhνのエネルギーを放出する。このことは、電子と正孔とが井戸層幅のIn組成の多い領域に局在化して、局在エキシトンを形成し、レーザの閾値の低下を助ける。閾値が下がり、出力が高くなるのはこの局在エキシトンの効果によるものである。さらに、この井戸層にSi等のn型不純物、Zn等のp型不純物をドーピングすることにより、伝導帯と価電子帯との間にさらに不純物レベルの準位ができる。図6BではSiと、Znとでもってその準位を示している。不純物をドーピングすると不純物レベルのエネルギー準位が形成される。そのため電子はより深い準位へ落ち、正孔はp型不純物のレベルに移動して、そこで電子と正孔とが再結合して、hν'のより小さいエネルギーを放出する。このことは電子と正孔とがさらに局在化することを意味し、この局在したエキシトン効果によりレーザの閾値が下がるのである。多数のピークが出現するのは、この局在エキシトンに加えて、三次元的に閉じ込められた量子箱の効果により多数の量子準位間の発光が出てくるからである。

【0020】n型不純物には、例えばSi、Ge、S_n、Se、Sを挙げることができる。p型不純物には、例えばZn、Cd、Mg、Be、Ca等を挙げることができる。これらの不純物を活性層中、特に好ましくは井戸層中にドーピングすることにより、量子準位間に、不純物レベルの発光を起こさせ、バンド間のエネルギー準位を小さくして、閾値を低下させることができる。なお、n型不純物、p型不純物両方をドーピングしてもよいことは言うまでもない。

【0021】特に好ましくはn型不純物、中でもSi、Geをドーピングすることにより、発光強度を強めると共に、閾値電流を低下させることができる。図4は井戸層にドーピングしたSi濃度と、閾値電流の低下率の割合を示す図である。具体的には平均膜厚30オングストロームのInGa_Nよりなる井戸層と、平均膜厚70オングストローム障壁とを5層積層した多重量子井戸構造の活性層を有するレーザ素子において、前記井戸層中にSiをドーピングした際のレーザ素子の閾値の低下の割合を示しており、図に示す各点は実際のSi濃度を示している。この図に示すようにSiをドーピングすることにより、閾値電流を最大で50%近く低下させることができる。従って、好ましいSi濃度は、 $1 \times 10^{18} / \text{cm}^3 \sim 1 \times 10^{22} / \text{cm}^3$ の範囲にあり、さらに好ましくは $5 \times 10^{18} / \text{cm}^3 \sim 2 \times 10^{21} / \text{cm}^3$ 、最も好ましくは $1 \times 10^{19} / \text{cm}^3$

$\sim 1 \times 10^{21} / \text{cm}^3$ である。なおこの図はSiについて示したものであるが、他のn型不純物、Ge、S_n等に対しても同様の傾向があることを確認した。

【0022】図5は井戸層にドーピングしたMg濃度と、閾値電流の低下率の割合を示す図である。これも同じく平均膜厚30オングストロームのInGa_Nよりなる井戸層と、平均膜厚70オングストローム障壁とを5層積層した多重量子井戸構造の活性層を有するレーザ素子において、前記井戸層中にMgをドーピングした際のレーザ素子の閾値の低下の割合を示しており、図に示す各点は実際のMg濃度を示している。この図に示すように、Mgをドーピングすることにより、閾値電流を25%近く低下させることができる。好ましいMg濃度は、 $1 \times 10^{17} / \text{cm}^3 \sim 1 \times 10^{22} / \text{cm}^3$ の範囲にあり、さらに好ましくは $1 \times 10^{18} / \text{cm}^3 \sim 2 \times 10^{21} / \text{cm}^3$ 、最も好ましくは $1 \times 10^{18} / \text{cm}^3 \sim 1 \times 10^{21} / \text{cm}^3$ である。なお、この図はMgについて示したものであるが、他のp型不純物、Zn、Cd、Be等に対しても同様の傾向があることを確認した。

【0023】

【実施例】以下、MOVPE法を用いて、図1に示す構造のレーザ素子を得る方法を説明する。図1は本発明のレーザ素子の一構造を示すものであって、本発明のレーザ素子はこの構造に限定されるものではない。なお本発明において示すIn_xGa_{1-x}N、Al_yGa_{1-y}N等の一般式は、単に窒化物半導体の組成式を示しているに過ぎず、異なる層が同一の式で示されていても、それらの層が同一の組成を示すものでは決してない。

【0024】[実施例1] サファイアのA面を主面とする基板1を用意し、この基板1をMOVPE装置の反応容器内に設置した後、原料ガスにTMG(トリメチルガリウム)と、アンモニアを用い、温度500℃でサファイア基板1の表面にGa_Nよりなるバッファ層2を200オングストロームの膜厚で成長させる。基板1にはA面の他にC面、R面等の面方位を有するサファイアが使用でき、サファイア他、スピネル111面(MgAl₂O₄)、SiC、MgO、Si、ZnO、Ga_N等の単結晶よりなる、公知の基板が用いられる。バッファ層2は基板と窒化物半導体との格子不整合を緩和するために設けられ、通常、Ga_N、Al_N、AlGa_N等が1000オングストローム以下の膜厚で成長されるが、窒化物半導体と格子定数の近い基板、格子整合した基板を用いる場合、成長方法、成長条件等の要因によっては成長されないこともあるので、省略することもできる。但し、サファイア、スピネルのように、窒化物半導体と格子定数が異なる基板を用いる場合、特開平4-297023号公報に記載されるように、200℃以上、900℃以下の温度でバッファ層2を成長させると、次に高温で成長させる窒化物半導体層の結晶性が飛躍的に良くなる。

【0025】続いて温度を1050℃に上げ、原料ガスにTMG、TMA（トリメチルアルミニウム）、アンモニア、ドナー不純物としてSiH₄（シラン）ガスを用いて、SiドープAl_{0.3}Ga_{0.7}Nよりなるn型コンタクト層3を4μmの膜厚で成長させる。

【0026】n型コンタクト層3は光閉じ込め層としても作用する。n型コンタクト層3をAlとGaを含むn型窒化物半導体、好ましくはn型Al_{1-y}Ga_yN（0<y<1）とすることにより、活性層との屈折率差が大きくでき、光閉じ込め層としてのクラッド層、及び電流を注入するコンタクト層として作用する。さらに、このコンタクト層をAl_yGa_{1-y}Nとすることにより、活性層の発光をn型コンタクト層内で広がりなくできるので、閾値が低下する。n型コンタクト層3をAl_yGa_{1-y}Nとする場合、基板側のAl混晶比が小さく、活性層側のAl混晶比が大きい構造、即ち組成傾斜構造とすることが望ましい。前記構造とすることにより、結晶性の良いn型コンタクト層が得られるので、結晶性の良いn型コンタクト層の上に積層する窒化物半導体の結晶性も良くなるため、素子全体の結晶性が良くなり、ひいては閾値の低下、素子の信頼性が格段に向上する。また活性層側のAl混晶比が大きいため、活性層との屈折率差も大きくなり光閉じ込め層として有効に作用する。また、このn型コンタクト層3をGa_{0.95}Nとしてもよい。Ga_{0.95}Nの場合、n電極とのオーミック特性については非常に優れている。コンタクト層をGa_{0.95}Nとすると、Ga_{0.95}Nコンタクト層と、活性層との間にAlGa_{0.95}Nよりなる光閉じ込め層を設ける必要がある。このn型コンタクト層3の膜厚は0.1μm以上、5μm以下に調整することが望ましい。0.1μm以下であると、光閉じ込め層として作用しにくく、また、電極を同一面側に設ける場合に、精密なエッチングレートの制御をせねばならないので不利である。一方、5μmよりも厚いと、結晶中にクラックが入りやすくなる傾向にある。

【0027】続いて、温度を1050℃に保持し、原料ガスにTMG、アンモニア、シランガスを用いて、Siドープn型Ga_{0.95}Nよりなるn型クラッド層4を500オングストロームの膜厚で成長させる。

【0028】このn型クラッド層4はn層側の光ガイド層、および活性層にInGa_{0.95}Nを成長させる際のバッファ層として作用し、n型Ga_{0.95}Nの他、n型InGa_{0.95}Nを成長させることもできる。バッファ層と成長させる場合には0.05μm以下の膜厚で成長させることが望ましい。また、前記のようにコンタクト層2をGa_{0.95}Nで成長させた場合、このn型クラッド層4は、光閉じ込め層として作用させるためにAlGa_{0.95}Nで成長させる必要がある。AlGa_{0.95}N層の場合、膜厚は0.01μm～0.5μmの膜厚で成長させることが望ましい。0.01μmより薄いと光閉じ込め層として作用しにくく、0.5μmよりも厚いと結晶中にクラックが入りやすい傾向にあ

る。

【0029】次に、温度を750℃にして、原料ガスにTMG、TMI（トリメチルインジウム）、アンモニア、不純物ガスとしてシランガスを用いてSiをドープした活性層5を成長させる。活性層5は、まずSiを1×10²⁰/cm³の濃度でドープしたIn_{0.2}Ga_{0.8}Nよりなる井戸層を25オングストロームの膜厚で成長させる。次にシランガスを止めて、TMIのモル比を変化させるのみで同一温度で、ノンドープIn_{0.01}Ga_{0.99}Nよりなる障壁層を50オングストロームの膜厚で成長させる。この操作を13回繰り返し、最後に井戸層を成長させ総膜厚0.1μmの多重量子井戸構造よりなる活性層5を成長させる。

【0030】活性層5は、少なくとも井戸層がInを含む窒化物半導体を含む多重量子井戸構造とする。多重量子井戸構造とは、井戸層と障壁層とを積層したものであり、本発明の場合、井戸層がInを含む窒化物半導体で構成されていれば、障壁層は井戸層よりもバンドギャップが大きければ特にInを含む必要はない。好ましくは、In_xGa_{1-x}N（0<x≤1）よりなる井戸層と、In_{x'}Ga_{1-x'}N（0≤x'<1、x'<x）よりなる障壁層とを積層した構造とする。三元混晶のInGa_{0.95}Nは四元混晶のものに比べて結晶性が良い物が得られるので、発光出力が向上する。また障壁層は井戸層よりもバンドギャップエネルギーを大きくして、井戸+障壁+井戸+・・・+障壁+井戸層（その逆でもよい。）となるように積層して多重量子井戸構造を構成する。井戸層の膜厚は70オングストローム以下、さらに望ましくは50オングストローム以下に調整することが望ましい。また障壁層の厚さも150オングストローム以下、さらに望ましくは100オングストローム以下の厚さに調整することが望ましい。井戸層が70オングストロームよりも厚いか、または障壁層が150オングストロームよりも厚いと、レーザ素子の出力が低下する傾向にある。このように活性層をInGa_{0.95}Nを積層したMQWとすると、量子準位間発光で約365nm～660nm間での高出力なLDを実現することができる。特に好ましい態様として、両方の層をInGa_{0.95}Nとすると、InGa_{0.95}Nは、Ga_{0.95}N、AlGa_{0.95}N結晶に比べて結晶が柔らかい。そのため第1のp型層であるAlGa_{0.95}Nの厚さを厚くできるのでレーザ発振が実現できる。またn型不純物は本実施例のように井戸層にドープしてもよいし、また障壁層にドープしてもよく、さらに井戸層、障壁層両方にドープしてもよい。

【0031】活性層5の膜厚は、n型コンタクト層3をAl_yGa_{1-y}Nとした場合、200オングストローム以上、さらに好ましくは300オングストローム以上の膜厚で成長させることが望ましい。なぜなら、MQWよりなる活性層を厚く成長させることにより、活性層の最外層近辺が光ガイド層として作用する。つまり、n型コン

タクト層3と第3のp型層8とが光閉じ込め層として作用し、活性層の最外層近傍が光ガイド層として作用する。活性層の膜厚の上限は特に限定するものではないが、通常は0.5 μ m以下に調整することが望ましい。

【0032】次に、原料ガスにTMG、TMA、アンモニア、p型不純物としてCp2Mg（シクロペンタジエニルマグネシウム）を用いて、Mgドープp型Al0.2Ga0.8Nよりなる第1のp型層6を100オングストロームの膜厚で成長させる。

【0033】第1のp型層6はAlを含むp型の窒化物半導体で構成し、好ましくは三元混晶若しくは二元混晶のAl_{1-y}Ga_{1-y}N（0<y≤1）を成長させることが望ましい。さらに、このAlGa_{1-y}Nは後に述べる第3のp型層8よりも膜厚を薄く形成することが望ましく、好ましくは10オングストローム以上、0.5 μ m以下に調整する。この第1のp型層6を活性層5に接して形成することにより、素子の出力が格段に向上する。これは、第1のp型層6成長時に、活性層のInGa_{1-y}Nが分解するのを抑える作用があるためと推察されるが、詳しいことは不明である。第1のp型層6は好ましく10オングストローム～0.5 μ m以下の膜厚で成長させることが望ましいが、省略することもできる。

【0034】次に、温度を1050℃にし、TMG、アンモニア、Cp2Mgを用いて、Mgドープp型Ga_{1-y}Nよりなる第2のp型層7を500オングストロームの膜厚で成長させる。

【0035】この第2のp型層7はp層側の光ガイド層若しくはバッファ層として作用し、好ましくは二元混晶または三元混晶のIn_yGa_{1-y}N（0≤y<1）を成長させる。第2のp型層7は、活性層の膜厚が薄い場合に成長させると光ガイド層として作用する。また第1のp型層6がAlGa_{1-y}N等よりなるので、この層がバッファ層のような作用をして、次に成長させる第3のp型層8をクラック無く結晶性良く成長できる。つまり、AlGa_{1-y}Nの上に直接バンドギャップが大きいAlGa_{1-y}Nを積層すると、後から成長させたバンドギャップが大きいAlGa_{1-y}Nにクラックが入りやすくなるので、この第2のp型層7を介することによりクラックを入りにくくしている。第2のp型層7は、通常100オングストローム～0.5 μ m程度の膜厚で成長させることが望ましいが、省略することもできる。

【0036】次に、温度を1050℃に上げ、原料ガスにTMG、TMA、アンモニア、アクセプター不純物としてCp2Mgを用いて、MgドープAl0.3Ga0.7Nよりなる第3のp型層8を0.3 μ mの膜厚で成長させる。

【0037】第3のp型層8は、Alを含む窒化物半導体で構成し、好ましくは二元混晶または三元混晶のAl_{1-y}Ga_{1-y}N（0<y≤1）を成長させる。第3のp型層8は、光閉じ込め層として作用し、0.1 μ m～1 μ m

の膜厚で成長させることが望ましく、AlGa_{1-y}NのようなAlを含むp型窒化物半導体とすることにより、好ましく光閉じ込め層として作用する。この第3のp型層も活性層5をInを含む窒化物半導体としているために、成長可能となる。つまり、InGa_{1-y}Nを含む活性層が緩衝層のような作用をするために、AlGa_{1-y}Nを厚膜で成長させやすくなる。逆にAlを含む窒化物半導体層の上に、直接光閉じ込め層となるような厚膜で、Alを含む窒化物半導体を成長させることは難しい傾向にある。

【0038】続いて、1050℃でTMG、アンモニア、Cp2Mgを用い、Mgドープp型Ga_{1-y}Nよりなるp型コンタクト層9を0.5 μ mの膜厚で成長させる。

【0039】p型コンタクト層9は電流を注入する層であり、p型の窒化物半導体（In_xAl_{1-y}Ga_{1-x-y}N、0≤x、0≤y、x+y≤1）で構成することができ、特にInGa_{1-y}N、Ga_{1-y}N、その中でもMgをドープしたp型Ga_{1-y}Nとすると、最もキャリア濃度の高いp型層が得られて、正電極と良好なオーミック接触が得られ、しきい値電流を低下させることができる。正電極の材料としてはNi、Pd、Ir、Rh、Pt、Ag、Au等の比較的仕事関数の高い金属又は合金がオーミックが得られやすい。

【0040】以上のようにして窒化物半導体を積層したウェーハを反応容器から取り出し、図1に示すように最上層のp型コンタクト層9より選択エッチングを行い、n型コンタクト層3の表面を露出させ、露出したn型コンタクト層3と、p型コンタクト層9との表面にそれぞれストライプ状の電極を形成した後、サファイア基板のR面からウェーハを劈開して、バー状にし、さらにストライプ状の電極に直交する方向にレーザの共振面を形成し、共振器長は600 μ mとする。後は、常法に従い、共振面に誘電体多層膜よりなる反射鏡を形成した後、ストライプ状の電極に平行な位置でウェーハを分割してレーザチップとする。このレーザチップをヒートシンクに設置し、順方向電流320mAのパルス発振を試みたところ、図3（c）に示すような不規則な位置に発光ピークを有するレーザ発振を示し、活性層に不純物をドープしていないレーザ素子に比較して、閾値電流は50%低下し、出力は30%向上した。

【0041】〔実施例2〕実施例1の活性層を成長させる工程において、不純物ガスとしてシランガスの代わりにジエチルジシランを用いて、Znを1×10¹⁹/cm³の濃度でドープしたIn0.2Ga0.8Nよりなる井戸層を25オングストローム、ノンドープIn0.01Ga0.95Nよりなる障壁層を50オングストロームの膜厚で成長させて、同じく総膜厚0.1 μ mの多重量子井戸構造よりなる活性層5を成長させる他は、同様にして、共振器長600 μ mのレーザ素子を得たところ、活性層に不純物をドープしていないレーザ素子に比較して、閾値電流は25%低下し、出力は10%向上した。

【0042】【実施例3】実施例1の活性層を成長させる工程において、不純物ガスとしてシランガス、およびジエチルジシランを用いて、Siを $1 \times 10^{20}/\text{cm}^3$ 、及びZnを $1 \times 10^{19}/\text{cm}^3$ の濃度でドーピングしたIn_{0.2}Ga_{0.8}Nよりなる井戸層を25オングストローム、ノンドーピングIn_{0.01}Ga_{0.99}Nよりなる障壁層を50オングストロームの膜厚で成長させて、同じく総膜厚0.1 μm の多重量子井戸構造よりなる活性層5を成長させる他は、同様にして、共振器長600 μm のレーザ素子を得たところ、活性層に不純物をドーピングしていないレーザ素子と比較して、閾値電流は60%低下し、出力は35%向上した。

【0043】

【発明の効果】以上説明したように、本発明のレーザ素子はその発光スペクトルに、従来のレーザ素子の縦モードの発光スペクトルとは全く異なる発光ピークを有することにより発光出力が向上する。さらに、活性層中にn型不純物、p型不純物がドーピングされていることにより、発光出力を低下させることなく閾値を低下させることができる。このため、発光出力が高く閾値の低いレーザ素子を実現することができる。また、本発明のレーザ素子を埋め込みヘテロ型、屈折率導波型、実効屈折率導波型等の横モードの安定化を図るレーザ素子とすることにより、さらに閾値電流が下がる可能性がある。

【図面の簡単な説明】

【図1】 本発明の一実施例に係るレーザ素子の構造を示す模式断面図。

【図2】 図1のレーザ素子の活性層付近を拡大して示す模式断面図。

【図3】 本発明のレーザ素子にパルス電流を流した際の発光スペクトルを各電流値で比較して示す図。

【図4】 活性層にドーピングしたSi濃度と、レーザ素子の閾値電流の低下率との関係を示す図。

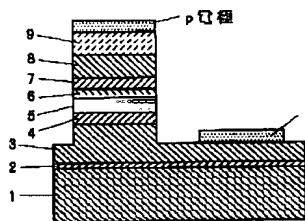
【図5】 活性層にドーピングしたMg濃度と、レーザ素子の閾値電流の低下率との関係を示す図。

【図6】 本発明のレーザ素子の井戸層のエネルギーバンド図。

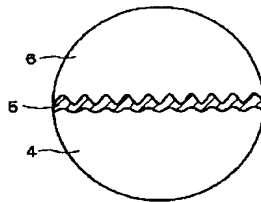
【符号の説明】

- 1・・・基板
- 2・・・バッファ層
- 3・・・n型コンタクト層
- 4・・・n型クラッド層
- 5・・・活性層
- 6・・・第1のp型層
- 7・・・第2のp型層
- 8・・・第3のp型層
- 9・・・p型コンタクト層

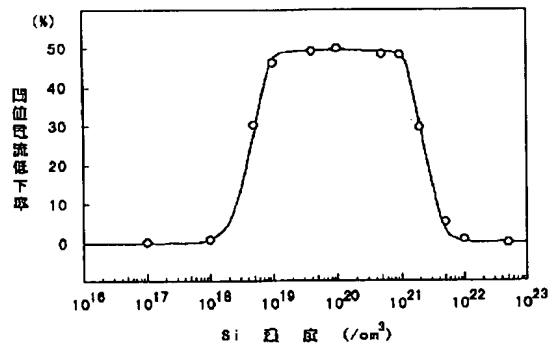
【図1】



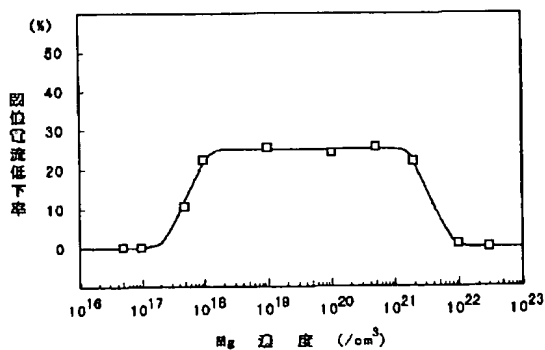
【図2】



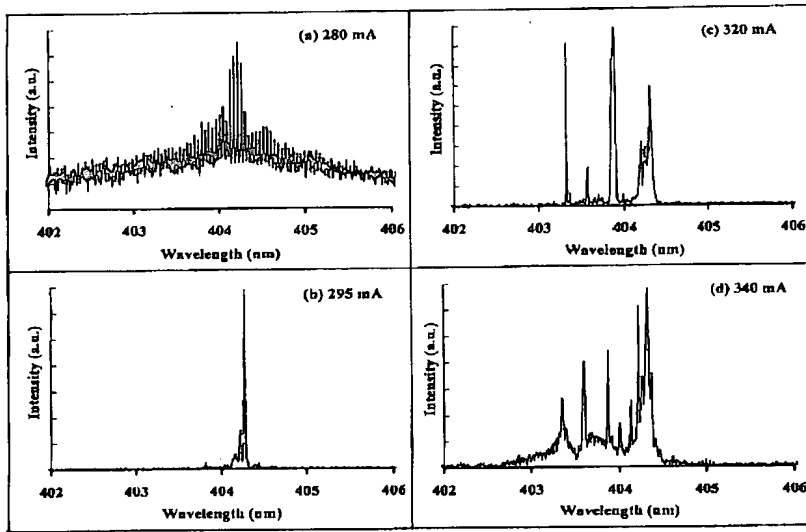
【図4】



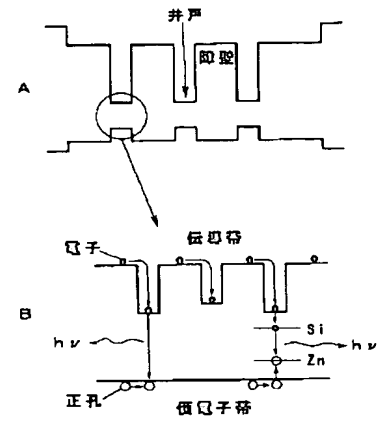
【図5】



【図3】



【図6】



SEMICONDUCTOR DEVICES

Physics and Technology

S.M. SZE
AT&T Bell Laboratories
Murray Hill, New Jersey

JOHN WILEY & SONS

New York

Chichester

Brisbane

Toronto

Singapore

Solution

At room temperature we assume that all donors are ionized; thus,

$$n \simeq N_D = 10^{16} \text{ cm}^{-3}.$$

From Fig. 7 we find $\rho = 0.48 \Omega\text{-cm}$. We can also calculate the resistivity from Eq. 15a

$$\rho = \frac{1}{qn\mu_n} = \frac{1}{1.6 \times 10^{-19} \times 10^{16} \times 1300} = 0.48 \Omega\text{-cm}.$$

The mobility μ_n is obtained from Fig. 3.

2.1.3 The Hall Effect

The carrier concentration in a semiconductor may be different from the impurity concentration, because the ionized impurity density depends on the temperature and the impurity energy level. To measure the carrier concentration directly, the most commonly used method is the Hall effect. Hall measurement is also one of the most convincing methods to show the existence of holes as charge carriers, because the measurement can give directly the carrier type. Figure 8 shows an electric field applied along the x -axis and a magnetic field applied along the z -axis. Consider a p -type semiconductor sample. The Lorentz force $q\mathbf{v} \times \mathbf{B}$ ($= qv_x B_z$) due to the magnetic field will exert an average upward force on the holes flowing in the x -direction. The upward-directed current causes an accumulation of holes at the top of the sample that gives rise to a downward-directed electric field \mathcal{E}_y . Since there is no net current flow along the y -direction in the steady state, the electric field along

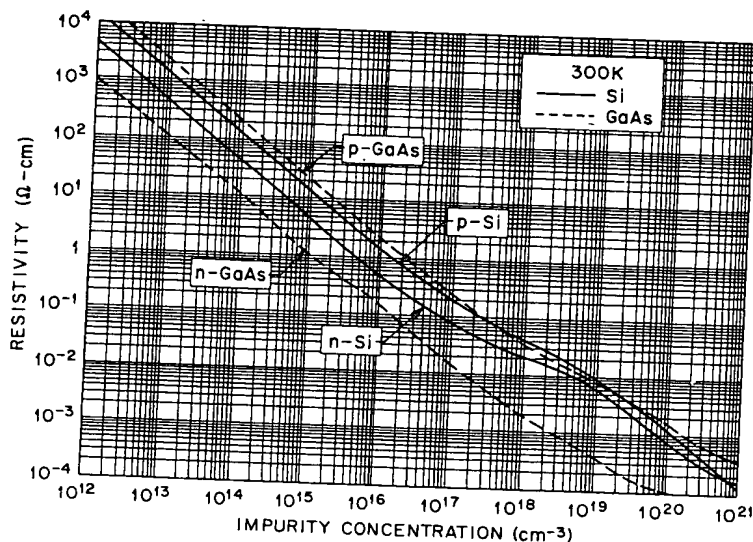


Fig. 7 Resistivity versus impurity concentration⁴ for Si and GaAs.

2.1 Carrier Drift

the y -axis exactly balance

or

Once the electric field \mathcal{E} direction is experienced t

The establishment of t
tric field in Eq. 18 is calle
(Fig. 8) is called the *Hall*
Hall field \mathcal{E}_y in Eq. 18 be

where

The Hall field \mathcal{E}_y is propo
magnetic field. The propo
lar result can be obtained
coefficient is negative:

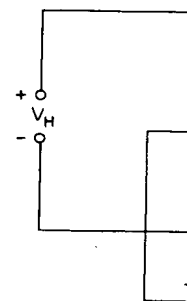


Fig. 8 Basic setup to

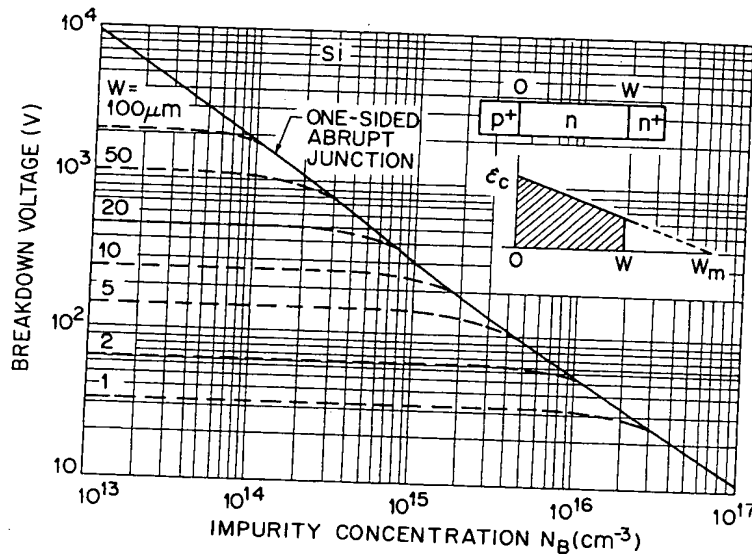


Fig. 27 Breakdown voltage for p^+-n-n^+ and p^+-p-n^+ junctions. W is the thickness of the lightly doped p -type (π) or the lightly doped n -type (ν) region.

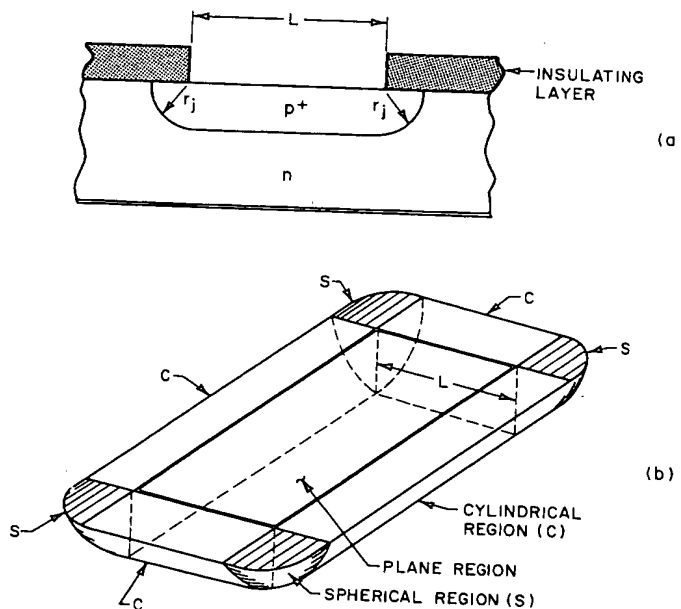


Fig. 28 (a) Planar diffusion process that forms junction curvature near the edge of the diffusion mask, where r_j is the radius of curvature. (b) Formation of cylindrical and spherical regions by diffusion through a rectangular mask.

References

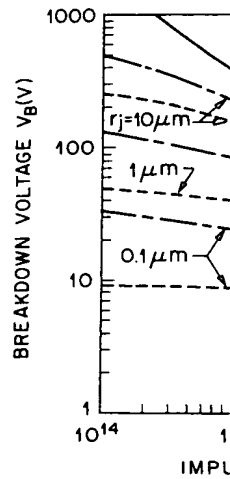
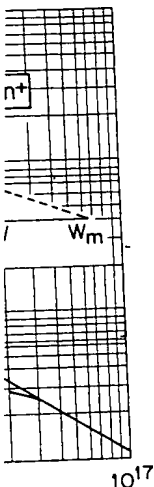


Fig. 29 Breakdown voltage versus profile with cylindrical and spherical curvature as indicated in Fig. 28.

roughly spherical shape show cal regions of the junction h. avalanche breakdown voltag abrupt junctions are shown. junctions considered previous smaller, the breakdown voltag junctions at low impurity conc

REFERENCES

- 1 W. Shockley, *Electrons and* 1950.
- 2 A. S. Grove, *Physics and Tec* 1967.
- 3 R. H. Kingston, "Switching" *Proc. IRE*, **42**, 829 (1954).
- 4 J. L. Moll, *Physics of Semicon*
- 5 S. M. Sze and G. Gibbons, *Linearly Graded p-n Junction* (1966).
- 6 S. K. Ghandhi, *Semiconductor*
- 7 S. M. Sze and G. Gibbons, "I in Semiconductors," *Solid Sta*
- 8 S. M. Sze, *Physics of Semiconc*



n^{-3}
W is the thickness of

ATING
R

(a)



(b)

CAL
3)

near the edge of the dif-
cylindrical and spherical

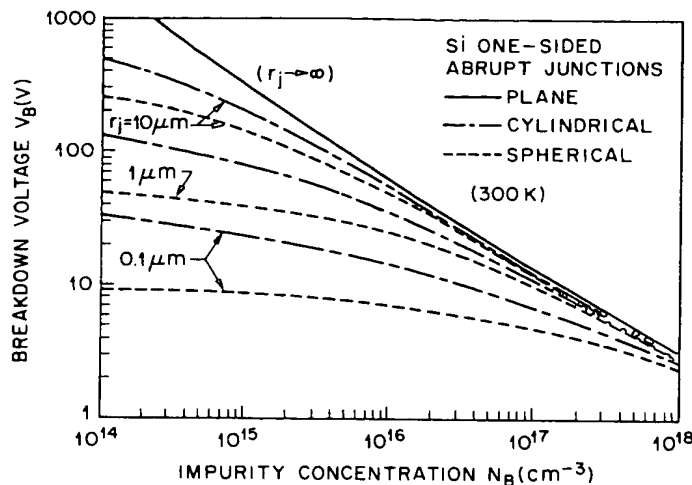


Fig. 29 Breakdown voltage versus impurity concentration for one-sided abrupt doping profile with cylindrical and spherical junction geometries,⁷ where r_j is the radius of curvature as indicated in Fig. 28.

roughly spherical shape shown in Fig. 28b. Because the spherical or cylindrical regions of the junction have a higher field intensity, they determine the avalanche breakdown voltage. The calculated results for silicon one-sided abrupt junctions are shown in Fig. 29. The solid line represents the plane junctions considered previously. Note that as the junction radius r_j becomes smaller, the breakdown voltage decreases dramatically, especially for spherical junctions at low impurity concentrations.

REFERENCES

1. W. Shockley, *Electrons and Holes in Semiconductors*, Van Nostrand, Princeton, 1950.
2. A. S. Grove, *Physics and Technology of Semiconductor Devices*, Wiley, New York, 1967.
3. R. H. Kingston, "Switching Time in Junction Diodes and Junction Transistors," *Proc. IRE*, **42**, 829 (1954).
4. J. L. Moll, *Physics of Semiconductors*, McGraw-Hill, New York, 1964.
5. S. M. Sze and G. Gibbons, "Avalanche Breakdown Voltages of Abrupt and Linearly Graded p-n Junctions in Ge, Si, GaAs and GaP," *Appl. Phys. Lett.*, **8**, 111 (1966).
6. S. K. Ghandhi, *Semiconductor Power Devices*, Wiley, New York, 1977.
7. S. M. Sze and G. Gibbons, "Effect of Junction Curvature on Breakdown Voltages in Semiconductors," *Solid State Electron.*, **9**, 831 (1966).
8. S. M. Sze, *Physics of Semiconductor Devices*, 2nd ed., Wiley, New York, 1981.



Fig. 10. (a) Active regions forward-biased.

base the hole density $p = 0$ and thus reduce I_C to zero.

Impurity distribution in a real device fabricated by epitaxial growth is not uniform but has a gradient, the electric field diagram is shown in Fig. 11. However, in thermal equilibrium the neutral base to collector electric field will push the holes to the emitter. In the same electric field biasing condition, the electric field is also due to diffusion but also

the time needed for the holes to turn around will improve the carrier recombination in the next section. Improvement of the base carrier recombination, less time in the base for electrons there. Impurities in the neutral

(38)

oped base region. If we use the equations, for exam-

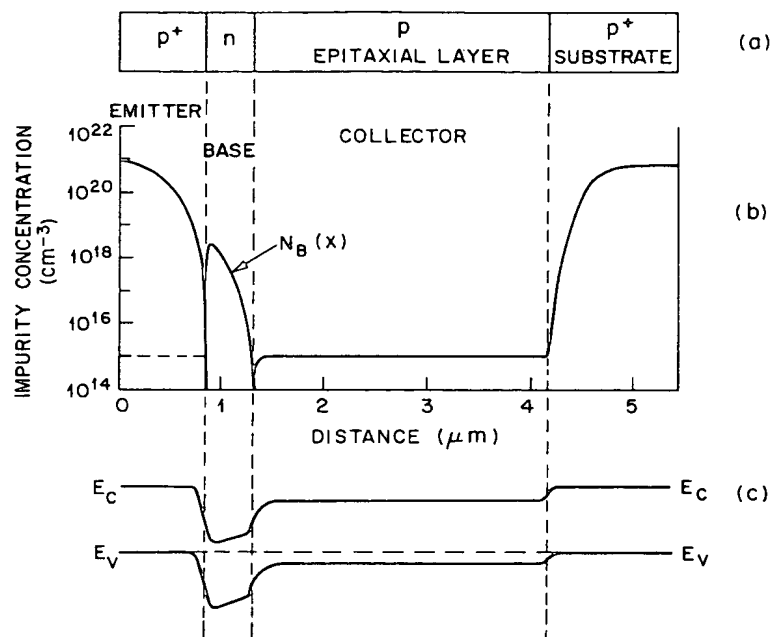


Fig. 11 (a) Cross-sectional view of a diffused bipolar transistor. (b) Impurity distribution in the transistor. (c) Corresponding band diagram in thermal equilibrium.

ple, Eqs. 28, 29, 31, 32, and 35a, results obtained for the ideal transistor can be readily adapted to diffused or ion-implanted transistors.

Base Resistance To achieve high current gain, the base width must be very narrow. Therefore, the base resistance can be quite high. Figure 12a shows a cross section of a $p-n-p$ transistor with two base contacts, one on each side of the emitter. The electrons are supplied from the base contacts and flow toward the center of the emitter causing the base-emitter voltage drop to vary with position along the base-emitter junction. As a first-order approximation with reference to Fig. 12a, the forward bias of the emitter junction above point A is

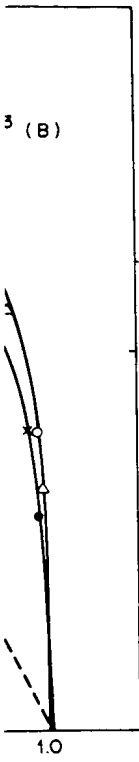
$$V_{EA} = V_{EB} - \frac{I_B}{2} (R_{AD} + R_{DB}). \quad (39)$$

The emitter bias voltage at point D is

$$V_{ED} = V_{EB} - \frac{I_B}{2} R_{DB} \quad (40)$$

which can be substantially larger than V_{EA} if R_{AD} is large.

Because the forward bias is largest at the edge of the emitter (point D), the recombination of holes will be greatest there. Therefore, most of the emitter current



silicon.⁸ The erfc distribu-

with the doubly charged
at high concentration
profile of phosphorus
because of a *dissociation*
various surface concen-
When the surface con-
n region, the diffusion
n increases, the profile
(and c). At very high
indeed similar to that
 n_e , a kink occurs and
The concentration n_e
luction band. At this
(P^{2-}) dissociates to P^+ ,

10.2 Extrinsic Diffusion

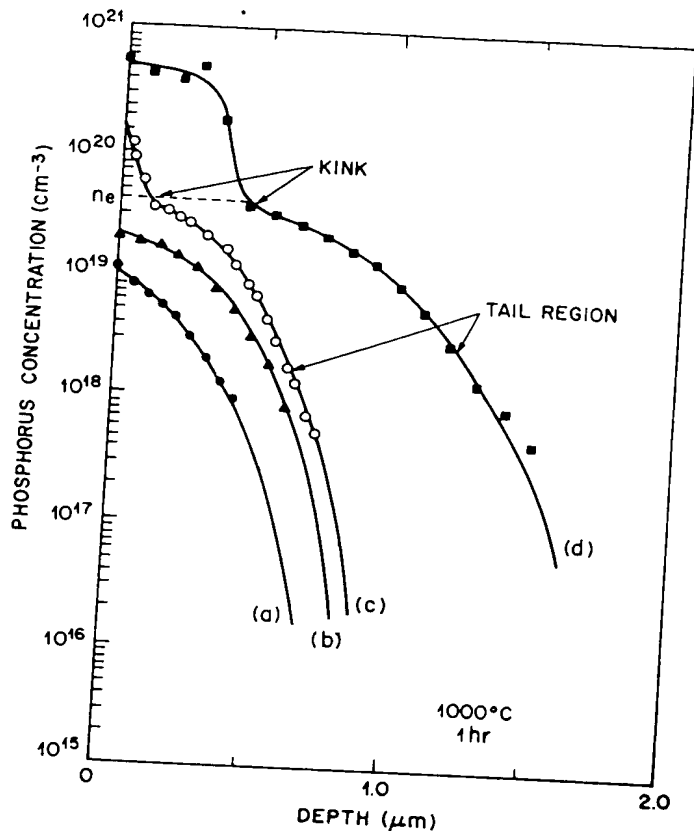


Fig. 11 Phosphorus diffusion profiles for various surface concentrations after diffusion into silicon for 1 hr at 1000°C.¹⁰

V^- , and an electron. Thus, the dissociation generates a large number of singly-charged acceptor vacancies V^- , which in turn enhance the diffusion in the tail region of the profile. The diffusivity in the tail region is over 10^{-12} cm²/s, which is about two orders of magnitude larger than the intrinsic diffusivity at 1000°C. Because of its high diffusivity, phosphorus is commonly used to form deep junctions such as the *n*-tubs in a CMOS.

Emitter-Push Effect In silicon *n-p-n* bipolar transistors using a phosphorus-diffused emitter and a boron-diffused base, the base region under the emitter region (inner base) is deeper by up to 0.6 μm than that outside the emitter region (outer base). This phenomena is called the *emitter push effect* and is illustrated in the insert of Fig. 12. The dissociation of phosphorus-vacancy (P^+V^{2-}) pairs at the kink region of the phosphorus profile (Fig. 11, curve *d*) provides a mechanism for the enhanced diffusion of phosphorus in the tail region. The diffusivity of boron under the emitter region (inner base)

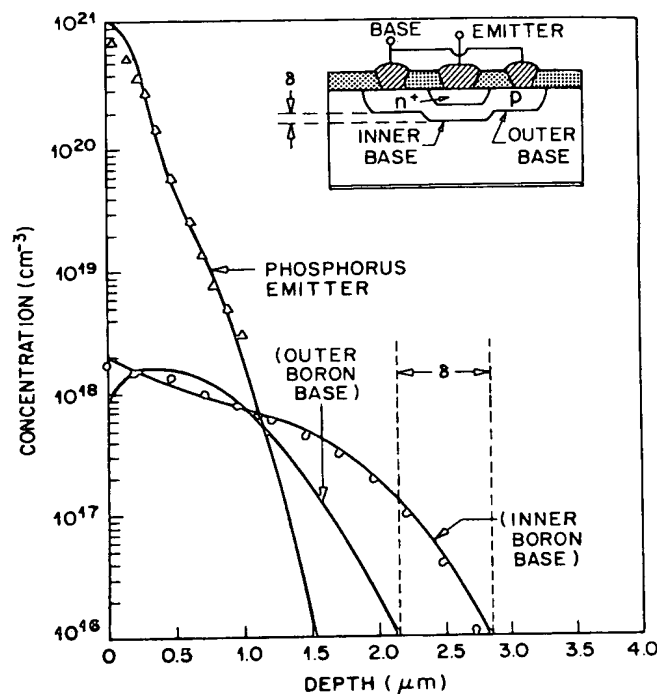


Fig. 12 Calculated and measured boron and phosphorus n - p - n transistor profile showing the emitter push effect. Emitter diffusion is at 1000°C , for 1 hr, followed by a 900°C , 45-min steam oxidation.⁸

also is expected to be enhanced by the dissociation of P^+V^{2-} pairs. Figure 12 shows close agreement between the measured profiles of boron and phosphorus and the calculated results (solid curves) based on the vacancy diffusion model.⁸

Zinc Diffusion in Gallium Arsenide The fundamental mechanisms for the diffusion of impurities in gallium arsenide have not yet been firmly established. We expect diffusion in gallium arsenide to be more complicated than that in silicon because the diffusion of impurities may involve atomic movements on both the gallium and arsenic sublattices. Vacancies play a dominant role in diffusion processes in gallium arsenide, because both p - and n -type impurities must ultimately reside in lattice sites; however, the charge states of the vacancies have not been established.

Zinc is the most extensively studied diffusant in gallium arsenide. Its diffusion coefficient is found to vary as C^2 . Therefore, the diffusion profiles are steep, as shown¹¹ in Fig. 13 and resembles curve b of Fig. 8. Note that even for the case of the lowest surface concentration, the diffusion is in the extrinsic-diffusion region, because n_i for GaAs at 1000°C is less than

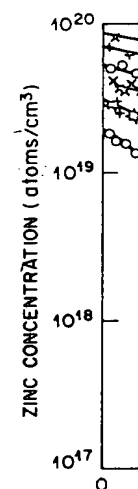


Fig. 13 Diffusion profile of zinc in gallium arsenide. The different surface temperatures in the range 1000 to 1100°C are indicated.

10^{18} cm^{-3} . As can be seen, the effect of the surface concentration of the zinc vapor on the junction pressure of the zinc is linearly proportional to the square root of the pressure.

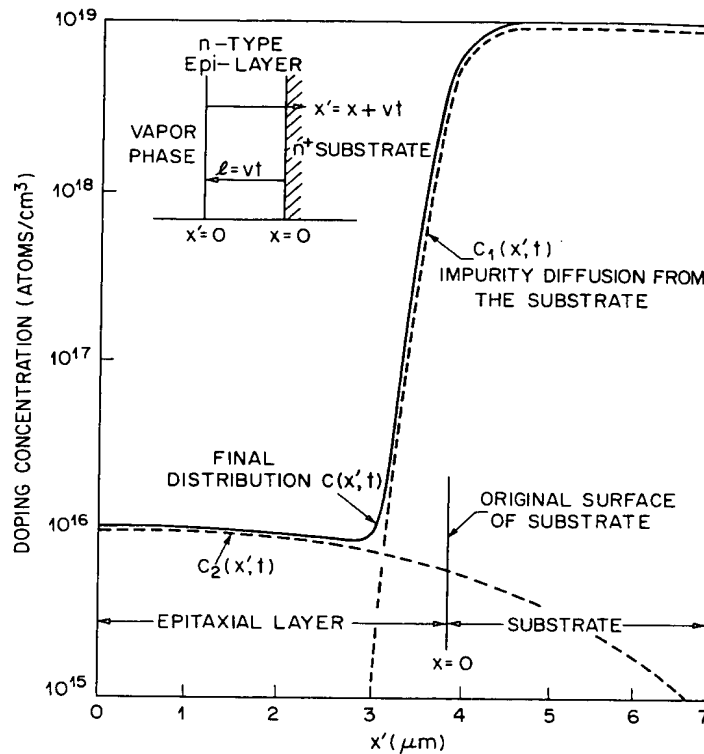
10.3 DIFFUSION-

In this section we discuss the important role of diffusion in the formation of a p - n junction.

10.3.1 Oxide N

The diffusivities of impurities in silicon dioxide are considerably smaller than in silicon. Silicon dioxide can be used as a passivation layer. It is important because it prevents the surface from being etched. If we etch windows in the oxide, we can incorporate dopants into the silicon to form p - n junctions.

For silicon dioxide, the diffusion of impurities is a two-step process. During the first step, the impurity diffuses in the form of P_2O_5 vapor. If the temperature continues, the thick oxide layer can be used to protect the silicon surface.

Fig. 17 Impurity redistribution during epitaxial growth.¹⁴

layer moves during growth, we require a solution to the problem of diffusion with a moving boundary.

The insert in Fig. 17 shows the geometry of the growth layer, where v is the epitaxial-layer growth rate (in cm/s). As the layer grows, the surface moves from the original substrate surface at the rate v . If we introduce a new variable $x' = x + vt$ into the diffusion equation (Eq. 4), we obtain

$$\frac{\partial C}{\partial t} = D \frac{\partial^2 C}{\partial x'^2} - v \frac{\partial C}{\partial x'} \quad (28)$$

If the original concentration in the substrate is C_1 and the concentration added to the epitaxial layer during growth is C_2 , the solution of Eq. 28 is

$$C(x', t) = \frac{C_2}{2} \left[\operatorname{erfc} \left[\frac{x' - vt}{2 \sqrt{D_2 t}} \right] + \exp \left[\frac{vx'}{D_2} \right] \operatorname{erfc} \left[\frac{x' + vt}{2 \sqrt{D_2 t}} \right] \right] + \frac{C_1}{2} \left[1 + \operatorname{erf} \left[\frac{x' - vt}{2 \sqrt{D_1 t}} \right] \right] \quad (29)$$

10.4 Distribution in a

where D_1 and D_2 are the diffusion coefficients in the epitaxial layer, and

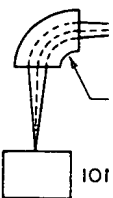
Figure 17 shows the impurity redistribution during epitaxial growth. The growth rate v is the rate at which the epitaxial layer moves. The contribution is obtained from $C_1(x', t)$ and $C_2(x', t)$. No impurity is added to the original substrate in this effect, which of course shows

10.4 DISTRIBUTION

Ion implantation into a substrate such as a semiconductor technology. Typical ion doses vary from 10^{12} to 10^{15} ions/cm². The main advantage is the reproducibility of the process. Requirements for the process include:

Figure 18 shows the ion source contains the ion source through a mass separator. The selected ions are accelerated to high energies by the vertical and horizontal deflection plates of the substrate.

VARIABLE
FOR BEAM
CONTROL



held at room temperature. Annealing temperature of the implanted ions are higher annealing even at 2×10^{15} boron or phosphorus at lower concentration. However, when the annealing temperature drops to about 550°C , the process is called *solid-phase epitaxy*. At this temperature, the surface layer becomes amorphous beneath the amorphous layer. The rate is 10 \AA/min at 550°C and 1 \AA/min at 500°C . Therefore, a 1000- to 2000-minute annealing is required. During the annealing, the ions are incorporated into the lattice and activation can be obtained.

The profile may be broadened by thermal annealing. A Gaussian distribution, also Gaussian.²⁵ Therefore, by Eq. 30 with ΔR_p^2 for thermal annealing, there is a relation between long annealing times and impurity concentrations become smaller, leading to minimize impurity concentration (ΔR_p). To achieve low-temperature annealing ($\sim 600^\circ\text{C}$) to remove the implantation damage.

It is studied using a variety of techniques — all short compared to the profiles for the ordinary furnace annealing. The e-beam annealing results show that minimal redistribution of the profile. Techniques where the power density is high and the annealing time is short. Also indicated are high-power techniques, and full dopant activation. Lower-power techniques for solid-phase epitaxy pro-

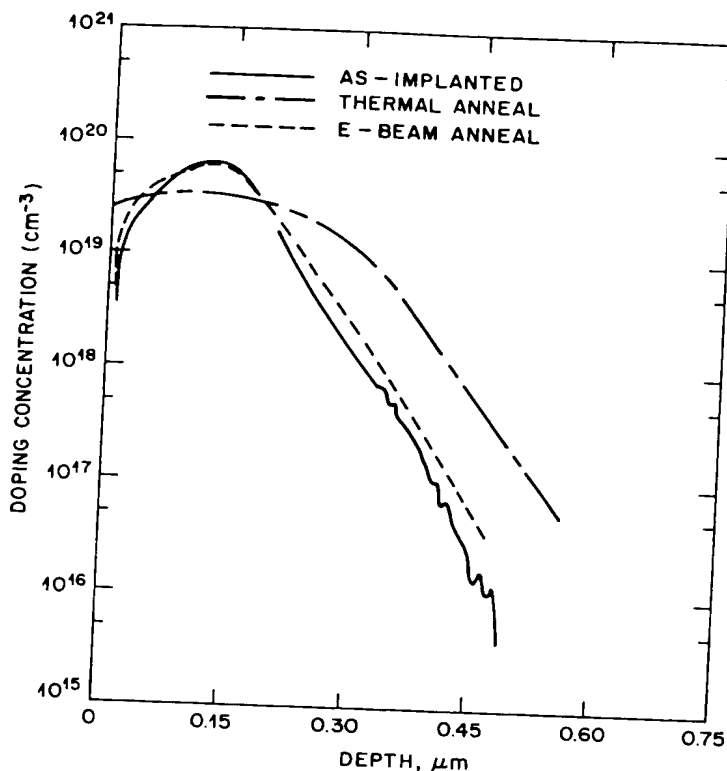


Fig. 31 Implanted boron concentration profile after an e-beam anneal and a thermal anneal.²⁴

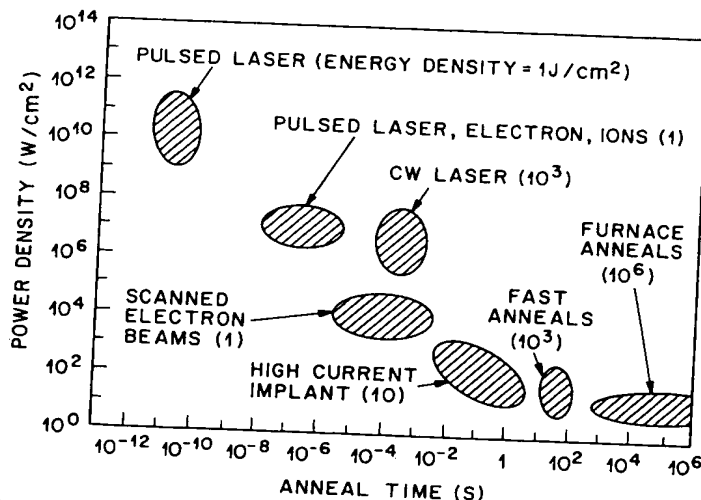


Fig. 32 Power density versus anneal time (pulse duration) for various short-time annealing techniques.²⁶

cess. Among these techniques, the most attractive are the *fast anneal* technique using broad-band spectral sources (e.g., incoherent light sources) and heating with an electron beam or ion beam, because the power densities required are lower and they produce no optical-interference effects. We expect that short-time annealing will eventually replace furnace annealing, especially for very-large-scale integrated circuits where dimensional controls of dopant distributions are critical.

10.6 IMPLANTATION-RELATED PROCESSES

In this section we consider a few implantation-related processes such as multiple implantation, masking, predeposition, threshold control, and pattern generation.

10.6.1 Multiple Implantation and Masking

In many applications doping profiles other than the simple Gaussian distribution are required. One such case is the pre-implantation of silicon with an inert ion to make the silicon surface region amorphous. This technique allows close control of the doping profile and permits nearly 100% dopant activation at low temperatures as discussed previously. In such a case, a deep amorphous region may be required. To obtain this type of region, we must make a series of implants at varying ion energies and doses.

Multiple implantation can also be used to form a flat doping profile as shown in Fig. 33. Here, four boron implants into silicon are used to provide a composite doping profile.²⁷ The measured carrier concentration and that predicted using range theory are shown in the figure. Other doping profiles,

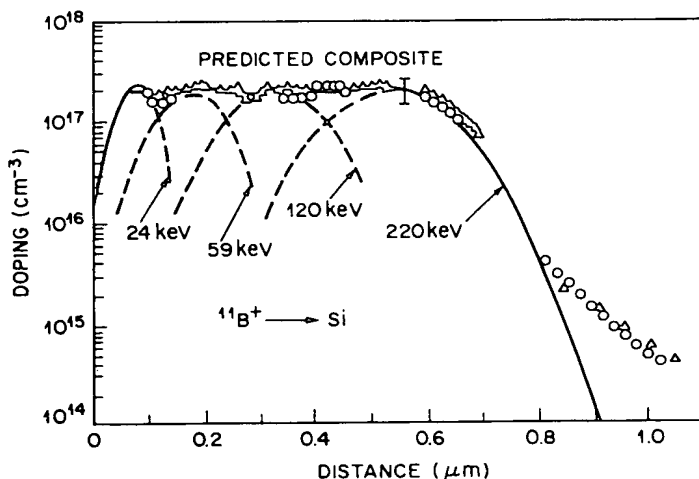


Fig. 33 Composite doping profile using multiple implants.²⁷

10.6 Implantation of n-Region

unavailable from diffusions of impurity

To form *p-n* junctions, appropriate mask should be used. The minimum thickness of incident ions is shown in the insert of Fig. 34 show implanted in the region of Eq. 30 as

$$S_d = -$$

From Table 1 we can

Therefore, the fraction

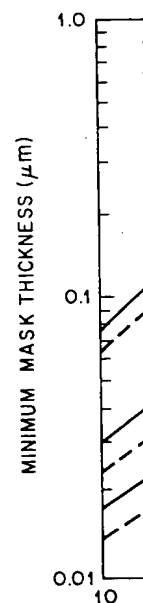


Fig. 34 Minimum thickness of mask. Insert shows ion penetration.

Electronics Engineers' Handbook

DONALD G. FINK *Editor*

Director Emeritus, Institute of Electrical and Electronics Engineers; Fellow, IEEE; Member of the National Academy of Engineering; Eminent Member, Eta Kappa Nu; Registered Professional Engineer; formerly Executive Director and General Manager, IEEE; Editor in Chief, Electronics; Vice President—Research, Philco Corporation; President, Institute of Radio Engineers; Editor, Proceedings of the IRE; Fellow of the Institution of Electrical Engineers (London)

DONALD CHRISTIANSEN *Editor*

Staff Director, Institute of Electrical and Electronics Engineers; Editor, IEEE Spectrum; Fellow, IEEE; Member, IEEE Publications Board; Eminent Member, Eta Kappa Nu; Member, New York Academy of Sciences; Member, Royal Institution (London); Fellow, World Academy of Art and Science; Registered Professional Engineer; formerly Editor in Chief, Electronics; Engineering Group Leader, CBS Electronics

Third Edition

McGRAW-HILL BOOK COMPANY

New York St. Louis San Francisco Auckland Bogotá
Hamburg London Madrid Mexico
Milan Montreal New Delhi Panama
Paris São Paulo Singapore
Sydney Tokyo Toronto

to have high current gain and high breakdown voltages. A device structure satisfying this requirement is one which uses a relatively thick epitaxial layer (typically 8 to 12 μm) in the resistivity range of 1 to 5 $\Omega\cdot\text{cm}$. Figure 8-26a shows the typical impurity profile for a monolithic *nnp* transistor suitable for linear IC applications.²⁵ In general, the base diffusion can be approximated by a *Gaussian* impurity profile, and the emitter by a complementary error function type of profile. Since the isolation diffusion does not directly contribute to the electrical characteristics of the device, it is not shown separately in the figure.

Note that the base width W_B is defined by the intersection of the base-emitter and the base-collector impurity contours. For typical *nnp* devices utilized in linear ICs, W_B is of the order of 0.5 to 1 μm , with a typical control tolerance of $\pm 0.1 \mu\text{m}$.

In digital circuit applications where high switching speeds and low saturation voltages are needed, and where low breakdown voltages ($\leq 20 \text{ V}$) can be tolerated, a somewhat different impurity profile is used.²⁶ A typical example of this is shown in Fig. 8-26b. A high-speed digital circuit transistor normally uses a thinner epitaxial collector region and shallow base and emitter diffusions. This choice is made to reduce the parasitic *sidewall* capacitances associated with the side portions of diffused regions.

In saturating logic circuits, a small quantity of gold is also diffused into the device structure. Gold atoms diffuse very rapidly through the entire silicon lattice and serve as recombination centers for free carriers in silicon. The net effect of gold doping is the reduction of minority-carrier lifetime, which in turn reduces the *storage time* or the *turnoff* delay associated with switching an *nnp* transistor from saturated operation to OFF condition.

35. *nnp* Device Layout. Figure 8-27 shows the lateral geometry and the structural cross section of a typical small-signal *nnp* transistor, having the impurity profile shown in Fig. 8-26a. Note that the vertical dimensions of the structural cross section are not drawn to scale.

The common-emitter current gain β is a function of collector I_C . Figure 8-28 shows the β -vs.- I_C

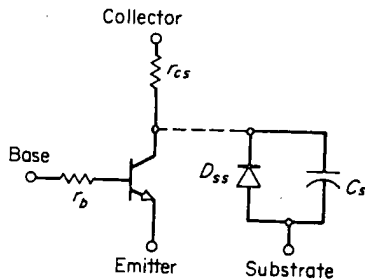


Fig. 8-25. Inherent parasitics associated with a junction-isolated transistor.

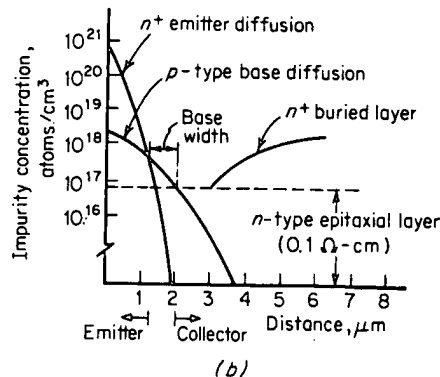
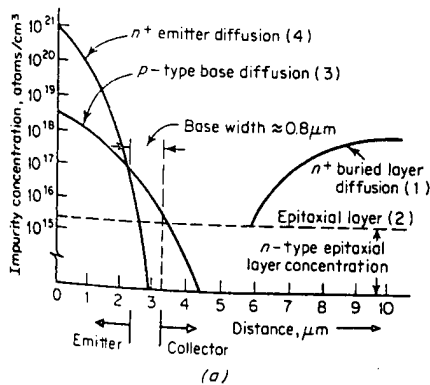


Fig. 8-26. Typical impurity profile for (a) linear-circuit transistor and (b) digital IC transistor.

characteristics for a typical small-signal *nnp* transistor, having the geometry of Fig. 8-27 and the impurity profile of Fig. 8-26a. Current-gain characteristics of various other types of monolithic bipolar transistors of comparable size and geometry are also shown in the figure for comparison.

The degradation of β at low current levels is due primarily to parasitic surface-recombination effects. Low-current β can be improved by additional surface-passivation steps (such as nitride passivation) and by minimizing the emitter periphery-to-area ratio.²⁷

At high current levels, transistor current gain degrades, due to two separate effects: (1) decrease of emitter efficiency and (2) current crowding at the emitter periphery. The emitter efficiency can be improved by increasing the emitter area, and the current-crowding effects can be minimized

Final test

and passive
a number of
onstraints of
its. The same
are fabricated
device struc-
: devices also

nolithic bipo-
is the starting

tor structures
is used as the



TS.

ickness is grown
low-resistivity

om the top sur-
r the integrated
g the collector
opside collector
introduces two
associated junc-

eristics. In lin-
general required

late the junction depth, we must know the background concentration N_B of the original wafer. Figure 4.8 gives the resistivity of n - and p -type silicon as a function of dopant concentration. The background concentration can be determined using this figure.

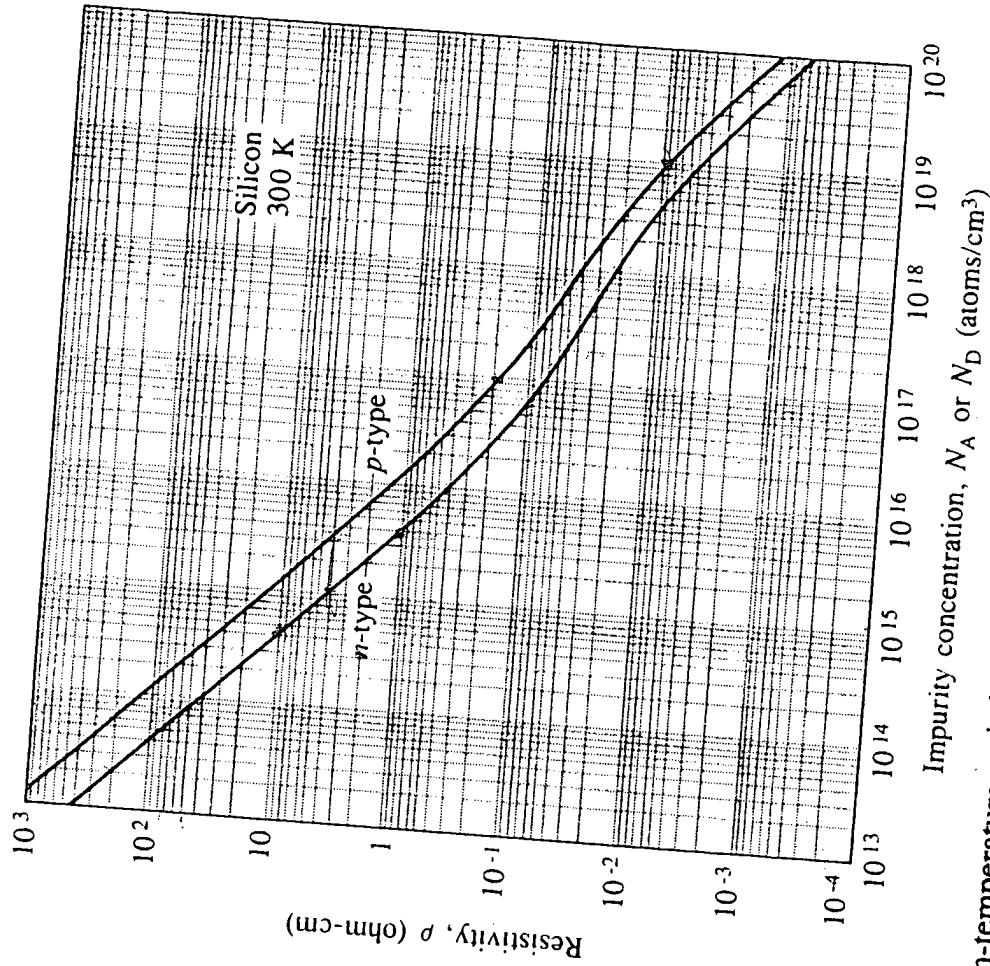


Fig. 4.8 Room-temperature resistivity in n - and p -type silicon as a function of impurity concentration. (Note that these curves are valid for either donor or acceptor impurities but not for compensated material containing both types of impurities.) Copyright 1987 Addison-Wesley Publishing Company. Reprinted with permission from ref. [3].

Carbon
Silicon
Resistivity
Impurity concentration
n-type
p-type
300 K